The SAS Chromatin-Remodeling Complex Mediates Inflorescence-Specific Chromatin Accessibility for Transcription Factor Binding

Jing Guo[a], Zhen-Zhen Liu[a], Yin-Na Su[a], Xin-Jian He[a,b*]

[a] National Institute of Biological Sciences, Beijing, 102206, China

[b] Tsinghua Institute of Multidisciplinary Biomedical Research, Tsinghua University, 100084, Beijing, China

[*] Corresponding author: Xin-Jian He (hexinjian@nibs.ac.cn)

Key words: chromatin remodeling; transcription factor; SWI/SNF; SAS; chromatin accessibility; flower development

Running title: Regulation of flower-specific chromatin accessibility

One-sentence summary: The SAS-type SWI/SNF complex regulates Inflorescence-specific chromatin accessibility at distal promoter and upstream intergenic regions, thereby facilitating the binding of transcription factors involved in flower development.

Abstract

While the role of transcription factors in flower development is well understood, the impact of chromatin remodeling on this process remains largely unclear. We conducted a comprehensive analysis to investigate the coordination of the SAS, BAS, and MAS-type SWI/SNF chromatin-remodeling complexes with transcription factors to regulate chromatin accessibility and gene transcription during flower development in *Arabidopsis thaliana*. Our findings indicate that the SAS complex binds to numerous genes related to flower development and is responsible for establishing chromatin accessibility of these genes during flower development. In contrast, the BAS and MAS complexes exhibit minimal involvement in regulating the accessibility of these genes. The SAS-bound genomic regions and the SAS-dependent accessible regions are enriched with sites occupied by multiple MADS family transcription factors involved in flower development. Furthermore, we found that the SAS-dependent accessibility is indispensable for the genomic binding of the MADS transcription factor AP1 at these regions. This study highlights the dynamic role of the SAS complex in modulating the genomic binding of transcription factors during plant development.

Introduction

Accurate gene expression in specific cells and developmental stages is crucial for the development of organisms. ATP-dependent chromatin-remodeling complexes play a vital role in facilitating the access of transcription factors and transcription machinery to DNA by utilizing the energy derived from ATP hydrolysis, thereby driving dynamic changes in gene expression. The SWI/SNF (Switch defective/Sucrose non fermentable) complex, originally discovered in yeast, was the first identified chromatin-remodeling complex (Cairns et al., 1994; Peterson et al., 1994). In *Drosophila melanogaster*, SWI/SNF components were found to be Trithorax group factors that counteract the repressive effect of Polycomb group proteins on the transcription of specific homeotic genes, ensuring the accurate expression of these homeotic genes at precise positions (Kennison and Tamkun, 1988; Tamkun et al., 1992). Moreover, extensive studies in

mammals have underscored the significance of SWI/SNF complexes in maintaining pluripotency and driving cell fate determination during development (Ho and Crabtree, 2010; Bieluszewski et al., 2023). Mutations in SWI/SNF subunits in humans have been closely linked to various types of tumors and developmental disorders (Cenik and Shilatifard, 2020).

In *Arabidopsis thaliana*, the SWI/SNF-type chromatin-remodeling ATPases consist of BRAHMA (BRM), SPLAYED (SYD), and MINUSCULE1/2 (MINU1/2). Some of the Arabidopsis SWI/SNF components were found to overcome the Polycomb repression (Wu et al., 2012; Li et al., 2015; Li et al., 2016; Shu et al., 2021), suggesting an evolutionarily conserved function of SWI/SNF complexes in plants and metazoans. Recent studies utilizing affinity purification followed by mass spectrometry (AP-MS) analysis have identified three classes of SWI/SNF complexes in Arabidopsis: the BRM-associated SWI/SNF (BAS) complex, the SYD-associated SWI/SNF (SAS) complex, and the MINU1/2-associated SWI/SNF (MAS) complex. Each of these complexes is composed of 8-15 subunits, with some subunits being specific to a particular complex, while others are shared by two or three complexes (Guo et al., 2022; Fu et al., 2023). However, the precise roles of different Arabidopsis SWI/SNF complexes in specific developmental processes remain elusive.

The effects of SWI/SNF components on plant growth and development have been extensively studied. Single mutants of *brm* and *syd*, as well as the weak *minu1/2* double mutant, display pleiotropic developmental defects, indicating the crucial role of SWI/SNF complexes in plant development. Moreover, the combination of *brm* and *syd* mutations, along with the *minu1/2* double knockout mutations, leads to lethality, further emphasizing the importance of these complexes (Wagner and Meyerowitz, 2002; Farrona et al., 2004; Bezhani et al., 2007; Sang et al., 2012). Notably, the mutants of BAS, SAS, and MAS components exhibit both overlapping and distinct phenotypes throughout Arabidopsis development (Bezhani et al., 2007; Guo et al., 2022). In particular, SAS-specific mutants, such as *syd*, *swi3d*, and *sys1/2/3*, consistently show

severe inflorescence developmental phenotypes, including defects in shoot meristem maintenance, splayed-opened sepals, dramatic homeotic transformation of floral organs, and complete sterility (Wagner and Meyerowitz, 2002; Kwon et al., 2005; Sarnowski et al., 2005; Guo et al., 2022). The BAS mutant *brm* also exhibits flower defects, including abnormal size and number of floral organs, homeotic transformation of the second and third flower whorls, fused filaments, and reduced fertility (Farrona et al., 2004; Hurtado et al., 2006). However, the floral homeotic defects in *brm* are generally milder compared to SAS-specific mutants (Guo et al., 2022). Additionally, other BAS-specific mutants, such as *swi3c*, *brip1/2*, and *brd1/2/13*, show weaker or nearly normal flower and silique phenotypes in comparison to *brm* (Archacki et al., 2009; Yu et al., 2020; Jaronczyk et al., 2021; Yu et al., 2021; Guo et al., 2022). Although MAS-specific mutants, including *minu1/2* and *pms2a/b*, have been reported to display abnormalities in the internal structures of flowers, shorter siliques, and reduced fertility, their sepals and petals develop normally (Sang et al., 2012; Diego-Martin et al., 2022; Guo et al., 2022). These studies suggest that SAS plays a more important role in flower development compared to BAS and MAS.

Flower development encompasses multiple stages, including floral induction, floral meristem formation, and floral organ development, which is a strictly controlled program regulated by a network of transcription factors, with the LEAFY (LFY) transcription factor and various MADS-box transcription factors playing crucial roles (Weigel, 1995). The genetic association between SWI/SNF components and flower development-related transcription factors was established over two decades ago when the *syd* mutation was found to enhance the floral homeotic defects in the weak *lfy* mutant (Wagner and Meyerowitz, 2002; Bieluszewski et al., 2023). In *brm* and *syd*, the expression of several floral homeotic genes is downregulated (Hurtado et al., 2006; Wu et al., 2012; Lin et al., 2023). It has been reported that LFY and the MADS-box transcription factor SEP3 recruit BRM and SYD to counteract Polycomb repression at the floral homeotic genes *AP3* and *AGAMOUS* (*AG*) during flower development (Wu et al., 2012). The AUXIN RESPONSE FACTOR (ARF) MONOPTEROS (MP) was

also reported to recruit BRM and SYD to increase the accessibility of its targets involved in flower formation upon auxin sensing (Wu et al., 2015). Additionally, the AP-MS results have demonstrated that BRM, SYD, and certain other SWI/SNF subunits are co-purified with multiple MADS transcription factors in flowers (Smaczniak et al., 2012), indicating interactions between SWI/SNF components and MADS transcription factors involved in flower development. A recent report has shown that LEAF AND FLOWER RELATED (LFR), a shared subunit of SAS and MAS, collaborates with the SAS catalytic subunit SYD to regulate the chromatin state and transcription of *AG* (Lin et al., 2023). These studies have mainly focused on the regulation of SWI/SNF components on specific genes associated with flower development. However, how the SWI/SNF complexes are coordinated with transcription factors to regulate gene transcription during flower development at the whole-genome level remains largely unclear.

In this study, we conducted a genome-wide analysis to compare the impact of BAS, SAS, and MAS complexes on chromatin accessibility and gene expression between seedlings and inflorescences. Our findings revealed that the SAS complex is responsible for establishing chromatin accessibility for a substantial subset of flower development-related genes in inflorescences as compared to seedlings. The SAS-bound genomic regions as well as the SAS-dependent accessible regions are enriched with genomic regions bound by MADS family transcription factors. The chromatin accessibility generated by SAS is required for the genomic binding of APETALA1 (AP1) at these regions. These results reveal the specific role of SAS in regulating the genomic binding of MADS transcription factors during flower development, providing insights into the molecular mechanism underlying the dynamic role of chromatin-remodeling complexes.

Results

SAS exhibits enhanced impact on gene expression in inflorescences relative to seedlings

134 We previously have determined the genome-wide effect of three classes of SWI/SNF
135 complexes on chromatin accessibility and gene expression in the seedlings (Guo et al.,
136 2022). However, whether and how the SWI/SNF complexes dynamically regulate
137 chromatin accessibility and gene expression in different development processes are
138 largely unclear. SAS mutants show several specific developmental phenotypes relative
139 to BAS and MAS mutants (Guo et al., 2022), a prominent phenotype among which is
140 the severe floral developmental defects (Supplemental Fig. S1A). In addition,
141 anthocyanin accumulation was also observed in the inflorescence stem and rosette
142 leaves of SAS mutants but not in BAS or MAS mutants (Supplemental Fig. S1, A and
143 B). To investigate the dynamic role of SWI/SNF complexes in regulating chromatin
144 accessibility and gene expression, we performed RNA deep sequencing (RNA-seq) in
145 the inflorescences and subsequently compared the effects of SWI/SNF mutations on
146 gene expression between the seedlings and the inflorescences. The SWI/SNF mutants
147 used in the RNA-seq analysis contain: the BAS mutant *brm*; the SAS mutants *syd*,
148 *swi3d*, and *sys1/2/3*; and the MAS mutants *minu1/2* and *pms2a/b*.

149 Multi-dimensional scaling (MDS) analyses of the RNA-seq data revealed a high
150 reproducibility of three biological replicates for the inflorescences of each genotype
151 (Fig. 1A). Based on the gene expression patterns, the mutants from the identical
152 SWI/SNF complex are clustered (Fig. 1B), confirming the reliability of the RNA-seq
153 data. We compared differentially expressed genes (DEGs) ($|\log2FC| \geq 1$ and $FDR < 0.05$)
154 detected in the seedlings and inflorescences of SWI/SNF mutants relative to the wild
155 type. Although the SAS mutants had the smaller number of DEGs compared to the BAS
156 and MAS mutants in seedlings (Guo et al., 2022), a significant increase of DEGs was
157 detected in the inflorescences of SAS mutants (Fig. 1C). Except for the weak *syd* mutant
158 allele, the two other SAS mutants *swi3d* and *sys1/2/3* had more DEGs than the BAS
159 and MAS mutants (Fig. 1C; Supplemental Fig. S1C; Supplemental Dataset 1), which is
160 consistent with the fact that the SAS mutants show more severe defects in the flower
161 development than the BAS and MAS mutants (Fig. 1D). This suggests that the SAS
162 complex plays a more important role in inflorescences than in seedlings. We compared

163 DEGs identified in the seedlings and inflorescences of each SWI/SNF mutant and found
164 that only a small portion of DEGs overlap between seedlings and inflorescences (Fig.
165 1, E-G; Supplemental Fig. S1, D-F), suggesting that the SWI/SNF complexes have a
166 dynamic role in regulating gene expression during development.

167 **Comparison of SWI/SNF-dependent accessibility between inflorescences and**
168 **seedlings**

169 Considering that the SWI/SNF complexes are mainly responsible for activating gene
170 expression by promoting chromatin accessibility (Clapier et al., 2017), and given that
171 the three classes of SWI/SNF complexes have been shown to facilitate genome-wide
172 chromatin accessibility in the seedlings (Guo et al., 2022), we determined chromatin
173 accessibility by performing the assay for transposase-accessible chromatin using
174 sequencing (ATAC-seq) and compared the effects of the SWI/SNF mutations on
175 chromatin accessibility between seedlings and inflorescences. On the basis of the
176 principal component analysis (PCA) of ATAC-seq data detected in the inflorescences,
177 the cluster of SAS mutants is more distant from the wild type than the BAS and MAS
178 mutants (Fig. 2A). Consistently, in the inflorescences, down-regulated differentially
179 accessible regions (DARs) identified in the SAS mutants are more abundant than those
180 in the BAS and MAS mutants (Fig. 2B; Supplemental Dataset 2). By comparing the
181 down-regulated differentially accessible regions identified in each SWI/SNF mutant
182 between seedlings and inflorescences, we found that the inflorescence-specific down-
183 regulated differentially accessible regions are also more abundant in the SAS mutants
184 than those in the BAS and the MAS mutants (Fig. 2C). The accessibility changes in
185 inflorescences are strongly correlated among the mutants of the same complex and are
186 weakly correlated among the mutants of different complexes (Fig. 2D). Specially, the
187 fold changes of accessibility in inflorescences are negatively correlated between the
188 SAS mutants and the MAS mutants (Fig. 2D), which is consistent with our previous
189 finding that SAS and MAS have antagonistic effects on regulating chromatin
190 accessibility in seedlings (Guo et al., 2022). These analyses suggest that the three

classes of SWI/SNF complexes regulate chromatin accessibility at different genomic regions and that SAS complex contributes more to chromatin accessibility than the other two types of SWI/SNF complexes in inflorescences.

Furthermore, we analyzed the distribution of the down-regulated differentially accessible regions in both seedlings and inflorescences of each SWI/SNF mutant and found that the distributions are overall identical between the seedlings and inflorescences (Supplemental Fig. S2, A and B; Supplemental Dataset 2). While the BAS and MAS-regulated accessible regions are enriched at the TSS-flanking regions, the SAS-regulated accessible regions are enriched at distal promoter regions and intergenic regions, which we hereafter refer to as distal accessible regions (Supplemental Fig. S2, A and B). In both seedlings and inflorescences, the SAS complex facilitates the accessibility at ~50% of distal accessible regions, whereas BAS and MAS mediate the accessibility only at < 10% of them (Supplemental Fig. S2C). In particular, the SAS complex contributes to chromatin accessibility at ~40% of the super enhancer regions defined by the top 2.5% of longest nonpromotor accessible region clusters in a previous study in Arabidopsis (Zhao et al., 2022), whereas the BAS and MAS complexes only show a marginal effect on the accessibility of the super enhancer regions (Supplemental Fig. S2D). These results point to the important role of SAS in promoting chromatin accessibility at distal accessible regions in both seedlings and inflorescences.

The ATAC-seq analysis indicated that the genes with decreased accessibilities are highly overlapped in different SAS mutants (Fig. 2E), suggesting the SAS components function together in regulating chromatin accessibility. Although the BAS and SAS complexes regulate chromatin accessibility primarily at different genomic regions (Fig. 2D; Supplemental Fig. S2, A and B), a substantial subset (~40%) of genes with down-regulated accessibility in the BAS mutant are shared by those with down-regulated accessibility in the SAS mutant (Fig. 2F). Given that the BAS and SAS can regulate the accessibility of the same set of target genes at proximal and distal regions, respectively

219 (Supplemental Fig. S2, A-C), the BAS and SAS complexes are likely to collaborate in
220 regulating the accessibility of different regions at a subset of their shared target genes.

221 **SAS regulates the accessibility and transcription of genes involved in flower**
222 **development**

223 We conducted a gene set enrichment analysis (GSEA) to examine genes with down-
224 regulated accessibility in the inflorescences of the BAS, SAS, and MAS mutants. We
225 found that flower-specific expressed genes exhibit enrichment among the genes with
226 down-regulated accessibility in the SAS mutant, and to a lesser extent in the BAS
227 mutant, whereas we did not observe this enrichment in the MAS mutant (Fig. 2, G-I;
228 Supplemental Fig. S3A). Consistently, the Gene Ontology (GO) analysis revealed a
229 significant enrichment of flower development-related genes among those exhibiting
230 down-regulated accessibility in the BAS and SAS mutants, and such enrichment was
231 not observed in the MAS mutants (Supplemental Fig. S3A; Supplemental Dataset 3).
232 Interestingly, the genes with down-regulated accessibility in the MAS mutants showed
233 enrichment in terms associated with protein targeting and metabolic processes
234 (Supplemental Fig. S3A; Supplemental Dataset 3). The housekeeping genes identified
235 by the previous study (Cheng et al., 2017) are significantly more enriched among genes
236 showing down-regulated accessibility in the MAS mutant than in the BAS and SAS
237 mutants (Supplemental Fig. S3B), suggesting that MAS shows the tendency to regulate
238 housekeeping genes but BAS and SAS avoid to regulate these genes. These results
239 indicate that SAS and BAS complexes but not the MAS complex are responsible for
240 promoting the accessibility of genes involved in flower development.

241 Among the genes with down-regulated accessibility in the inflorescences of each
242 SWI/SNF mutant, the DEGs are most abundant in the SAS mutants, followed by the
243 BAS mutant and then the MAS mutants (Fig. 2J). Moreover, the DEGs with decreased
244 expression were more abundant than those with increased expression in each SWI/SNF
245 mutant (Fig. 2J), supporting the notion that SWI/SNF-dependent accessibility primarily
246 functions in activating transcription rather than repressing it. It is noteworthy that most

247 of the genes with down-regulated accessibility in SWI/SNF mutants did not show
248 changes in expression (Fig. 2J), indicating that the SWI/SNF-dependent accessibility
249 contributes to establishing a priming chromatin state for transcription but is not
250 sufficient for actual transcription to occur. Taken together, these results suggest that
251 among the three classes of SWI/SNF complexes, the SAS complex plays a major role
252 in promoting chromatin accessibility and facilitating transcriptional activation during
253 flower development.

254 **SAS is responsible for establishing the accessibility of genes involved in flower**
255 **development**

256 The dynamic regulation of chromatin accessibility is involved in the regulation of gene
257 expression during flower development (Yan et al., 2019). To comprehensively
258 investigate the accessibility of genes involved in flower development at the whole-
259 genome level, we compared the chromatin accessibility between seedlings and
260 inflorescences based on our ATAC-seq results in the wild type. The ATAC-seq analysis
261 identified a total of 1,325 genes (corresponding to 1,842 peaks) with increased
262 accessibility and 1,344 genes (corresponding to 1,742 peaks) with decreased
263 accessibility in inflorescences compared to seedlings (Fig. 3A, Supplemental Dataset
264 4). The genes displaying increased accessibility in inflorescences were found to be
265 enriched with gene ontology (GO) terms associated with flower development
266 (Supplemental Fig. S4A). Conversely, the genes exhibiting decreased accessibility were
267 enriched with GO terms related to stress response (Supplemental Fig. S4B).

268 Next, we determined to what extent the SWI/SNF complexes contribute to the
269 accessibility of inflorescence-specific accessible genes, and found that > 50% of the
270 inflorescence-specific accessible genes were regulated by the SAS components, while
271 around 20% were regulated by the BAS or MAS components (Fig. 3B). In contrast, the
272 numbers of seedling-specific accessible genes regulated by BAS, SAS, and MAS were
273 not markedly different (Fig. 3C). Among the 1,325 inflorescence-specific accessible
274 genes, 47% (629/1,325) of them are overlapped with the 1,778 genes with decreased

accessibility in all the three tested SAS mutants (Fig. 3D). The GO analysis indicated that the 629 SAS-regulated, inflorescence-specific accessible genes (type I) are closely associated with flower development, whereas the remaining 696 inflorescence-specific accessible genes (type II) not regulated by SAS were enriched with the term ‘maintenance of cell number’, which is not directly related to flower development (Fig. 3E), confirming that SAS is specifically responsible for establishing flower-specific chromatin accessibility.

To characterize the accessible regions regulated by three classes of SWI/SNF complexes in both seedlings and inflorescences, we drew the average accessible signals at the 1,325 inflorescence-specific accessible genes and the 1,344 seedling-specific accessible genes in both wild-type plants and SWI/SNF mutants. For the inflorescence-specific accessible genes, we observed not only a TSS-flanking accessible region but also a distal accessible region upstream of the TSS (Fig. 3F, Supplemental Fig. S5A). This characteristic aligns with the typical feature of SAS-regulated accessible genes (Guo et al., 2022). However, the seedling-specific accessible genes do not exhibit this distinct 'SAS feature' (Fig. 3G; Supplemental Fig. S5B). SAS is the primary regulator required for the accessibility of inflorescence-specific accessible genes, whereas BAS, SAS, and MAS collectively contribute to the accessibility of seedling-specific genes (Fig. 3G; Supplemental Fig. S5B). It is worth noting that SAS weakly contributes to the accessibility of inflorescence-specific accessible genes in seedlings (Fig. 3F; Supplemental Fig. S5A). However, in wild-type plants, the accessibility of these genes is markedly lower in seedlings than in inflorescences (Fig. 3F; Supplemental Fig. S5A). Therefore, SAS contributes to chromatin accessibility at the distal promoter region of genes related to flower development.

Comparison of the binding patterns of BAS, SAS, and MAS in inflorescences and seedlings

To investigate the molecular mechanism underlying the different effects of SWI/SNF complexes on chromatin accessibility between seedlings and inflorescences, we

303 conducted chromatin immunoprecipitation followed by sequencing (ChIP-seq) for the
304 BAS subunit SWI3C, the SAS subunit SWI3D, and the MAS subunit PMS2B. We
305 observed that the replicates of the same sample are more correlated than different
306 samples (Supplemental Fig. S6A), indicating the reliability of our ChIP-seq results. The
307 results indicated that the binding peaks of the BAS and SAS subunits in both seedlings
308 and inflorescences formed a cluster with strong correlation, while displaying weak
309 correlation with the binding peaks of the MAS subunit (Fig. 4A). However, upon closer
310 examination, we found that the binding peaks of BAS and SAS subunits within the
311 same developmental stage exhibited higher correlation than one subunit across different
312 developmental stages (Fig. 4A), suggesting that BAS and SAS exhibited similar
313 distribution patterns in either seedlings or inflorescences, and their distributions showed
314 differences between the two developmental stages. Analysis of the binding peaks called
315 from the ChIP-seq data revealed that the three SWI/SNF complexes displayed a similar
316 number of binding peaks between seedlings and inflorescences (Fig. 4B; Supplemental
317 Dataset 5). Previous studies have indicated that, in seedlings, BAS and SAS share the
318 majority of their binding peaks, while most of the binding peaks of MAS are different
319 from those of BAS and SAS (Guo et al., 2022; Fu et al., 2023). The overlapping patterns
320 of BAS, SAS, and MAS peaks in inflorescences were similar to those in seedlings
321 (Supplemental Fig. S6B). However, whether and how the binding of SWI/SNF
322 complexes to chromatin is altered during plant development is largely unclear.

323 By comparing the binding peaks of each SWI/SNF subunit between seedlings and
324 inflorescences, we identified 1,023 BAS peaks, 1,415 SAS peaks, and 291 MAS peaks
325 exhibiting increased accumulation in inflorescences relative to seedlings, which we
326 termed inflorescence-specific binding peaks; and revealed 549 BAS peaks, 712 SAS
327 peaks, and 679 MAS peaks with decreased accumulation in inflorescences compared
328 to seedlings, which we termed seedling-specific binding peaks (Fig. 4C; Supplemental
329 Fig. S6, C-E; Supplemental Dataset 6). Although the three SWI/SNF complexes
330 showed similar numbers of seedling-specific binding peaks, the number of
331 inflorescence-specific binding peaks was significantly higher for SAS and BAS

332 compared to MAS (Fig. 4B). This suggests that the binding of SAS and BAS to
333 chromatin undergoes dynamic establishment during flower development. We assigned
334 the binding peaks to nearby genes and then defined the binding genes for the three
335 SWI/SNF complexes (Fig. 4, B and C), and found that the BAS and SAS-binding genes
336 were significantly overlapped among either inflorescence- or seedlings-specific binding
337 genes, whereas only a small portion of MAS-binding genes were overlapped with BAS
338 or SAS-binding genes (Supplemental Fig. 6, F and G). This was exemplified by the
339 binding signals of BAS, SAS, and MAS in seedlings and inflorescences at their random
340 target genomic regions (Fig. 4D). These results suggest that the binding of BAS and
341 SAS to chromatin is altered during development at a substantial subset of their target
342 loci.

343 Furthermore, we determined whether the distribution of the binding peaks for each
344 SWI/SNF complex across the genic region is altered in inflorescences compared to that
345 in seedlings, and found that the overall distribution of total binding peaks for each
346 SWI/SNF complex is similar between inflorescences and seedlings (Supplemental Fig.
347 S6H). However, the proportion of the SAS and BAS-binding peaks in intergenic and
348 distal promoter regions exhibited a slight increase in inflorescences relative to seedlings
349 (Supplemental Fig. S6H). Upon comparing the distributions of inflorescence-specific
350 SAS-binding regions and seedling-specific SAS-binding regions, we observed that SAS
351 has a higher tendency to bind intergenic and distal promoter regions in inflorescences
352 than in seedlings (Fig. 4E). The GO analysis revealed that the inflorescence-specific
353 SAS-binding genes are primarily associated with flower development, while the
354 seedling-specific SAS-binding genes are enriched in terms of stress response (Fig. 4, F
355 and G). These results suggest that the SAS is specifically recruited to a subset of genes
356 involved in flower development during the reproductive phase, rather than maintaining
357 a constant association with these genes between the vegetative and reproductive
358 processes.

359 **Recruitment of SAS establishes the accessibility of flower-development genes**

360 To determine the impact of BAS, SAS, and MAS binding on gene accessibility in
361 inflorescences and seedlings, we examined the genes specifically bound by each
362 complex in either inflorescences or seedlings and compared them to genes that
363 exhibited decreased accessibility in the corresponding complex mutant. Interestingly,
364 we found that inflorescence-specific SAS-binding genes showed the highest proportion
365 of accessibility changes compared to the inflorescence-specific BAS- and MAS-
366 binding genes (Fig. 5A). It is worth noting that although the numbers of inflorescence-
367 specific binding genes were comparable for BAS and SAS, the proportion of genes with
368 down-regulated accessibility was significantly lower in the BAS mutant (95/805) than
369 in the SAS mutant (382/1,071). This discrepancy in accessibility changes between the
370 BAS and SAS mutants might be attributed to the different remodeling activities of the
371 two complexes at their target regions. Further examination of SAS-specific binding
372 regions in inflorescences revealed that the regions with decreased accessibility
373 exhibited higher binding and accessibility signals compared to regions with maintained
374 accessibility (Fig. 5, B and C). This suggests that the enhanced binding affinity of SAS
375 at specific binding regions in inflorescences promotes the remodeling activity, leading
376 to increased accessibility.

377 To identify inflorescence-specific accessible genes that are specifically bound and
378 remodeled by SAS, we conducted an overlap analysis between the 382 SAS-specific
379 binding genes with decreased accessibility in the SAS mutant inflorescences (Fig. 5A)
380 and the 1,325 inflorescence-specific accessible genes (Fig. 3A). Remarkably, we found
381 that 61% (234/382) of the genes specifically bound and remodeled by SAS in
382 inflorescences were inflorescence-specific accessible genes, accounting for 18%
383 (234/1,325) of the total inflorescence-specific accessible genes (Fig. 5D). This subset
384 includes crucial flower development-related genes, such as *LFY* (Schultz and Haughn,
385 1991), *SEP2/3/4* (Pelaz et al., 2000; Ditta et al., 2004), *SAUR*s (Stortenbeker and Bemer,
386 2019), and *SPL*s (Chen et al., 2010) (Fig. 5D). Snapshots illustrating the association
387 between SWI/SNF binding and SWI/SNF-dependent accessibility at representative
388 genes are provided (Fig. 5E). These analyses highlight the contribution of SAS

389 recruitment to the establishment of accessibility for flower development-related genes
390 during flower development. Additionally, we discovered that 16% (211/1,325) of the
391 inflorescence-specific accessible genes exhibited SAS-dependent accessibility but were
392 bound by SAS in both inflorescences and seedlings (Fig. 5E), suggesting that the
393 involvement of SAS in inflorescence-specific accessibility is also regulated after SAS
394 is recruited to its target genes.

395 Furthermore, we investigated whether the SAS complex is involved in the expression
396 of flower development-related genes. We found that the accessibility of inflorescence-
397 specific accessible regions is significantly lower in the SAS mutant than in the wild-
398 type in the inflorescences (Supplemental Fig. S7A), confirming that the SAS complex
399 is crucial for facilitating the accessibility of the flower development-related genes
400 specifically in inflorescences. As determined by our RNA-seq data, the expression
401 levels of inflorescence-specific accessible genes are significantly higher in
402 inflorescences than in seedlings, and their expression levels are reduced in the SAS
403 mutant compared to the wild-type in inflorescences (Supplemental Fig. S7B). In the
404 SAS mutant, the inflorescence-specific accessible genes with decreased expression are
405 more abundant than those with increased expression (Supplemental Fig. S7C). These
406 results suggest that the SAS complex contributes to chromatin accessibility and thereby
407 facilitates the transcription of flower development-related genes. However, we also
408 found that the expression levels of a substantial subset of inflorescence-specific
409 accessible genes are not significantly reduced in the SAS mutant (Supplemental Fig.
410 S7C). Therefore, the SAS-dependent chromatin accessibility observed in inflorescences
411 may result in transcription occurring exclusively in specific cells and developmental
412 stages, and these localized transcriptional events may not be detectable in the RNA-seq
413 analysis of mixed inflorescence tissues.

414 **SAS-dependent accessible regions and transcription factors**

415 Similar to seedlings, where most SWI/SNF-regulated accessible regions are direct
416 targets of SWI/SNF complexes (Guo et al., 2022), we observed that in the

417 inflorescences of SWI/SNF mutants, the majority of accessible regions with decreased
418 accessibility are also directly bound by their corresponding SWI/SNF complexes (Fig.
419 6A). Out of the 3,972 accessible regions with decreased accessibility detected in *swi3d*
420 inflorescences, 60% of them are bound by SAS. Specifically, 14% of these regions are
421 exclusively bound by SAS in inflorescences, while 46% are bound by SAS in both
422 seedlings and inflorescences (Fig. 6B). Comparison of the inflorescence-specific SAS-
423 binding regions with the shared SAS-binding regions in seedlings and inflorescences
424 revealed that the inflorescence-specific regions exhibit higher SAS-binding signals and
425 lower accessibility signals (Fig. 6, C and D). It is important to note that the
426 inflorescence-specific binding of SAS to its target loci only accounts for a small subset
427 of SAS-dependent accessible regions (Fig. 6B). This further supports the notion that
428 the regulation of SAS-dependent accessibility in inflorescences involves additional
429 downstream steps following the binding of SAS to its target loci.

430 Previous studies have demonstrated that transcription factors either recruit SWI/SNF
431 complexes to specific target genes or collaborate with SWI/SNF to regulate chromatin
432 accessibility and transcriptional activation (Bieluszewski et al., 2023). In order to
433 investigate how SAS-dependent chromatin accessibility is regulated during flower
434 development, we examined whether the inflorescence-specific SAS-binding regions are
435 enriched with any transcription factor-binding DNA motifs. Interestingly, we found that
436 the inflorescence-specific SAS-binding regions are significantly enriched with the
437 DNA motifs bound by MADS and SBP transcription factors (Fig. 6E; Supplemental
438 Dataset 7). Given that the MADS and SBP transcription factors are important for flower
439 development (Chen et al., 2010; Theißen et al., 2016), it is likely that these transcription
440 factors either facilitate the recruitment of SAS to flower development-related genes or
441 collaborate with SAS to regulate the accessibility and/or transcription of these genes.
442 To further explore the relationship between SAS and the MADS-family transcription
443 factors, we compared the inflorescence-specific SAS-binding regions with the MADS-
444 binding regions previously identified in inflorescences or seedlings (Chen et al., 2018;
445 van Mourik et al., 2023). The analysis indicated that the inflorescence-specific SAS-

446 binding regions exhibited a high level of overlap (15%~50%) with the regions bound
447 by multiple MADS transcription factors in inflorescences, whereas the overlap (<10%)
448 was markedly reduced when they are compared with the regions bound by the MADS
449 transcription factors detected in seedlings (Fig. 6F). These findings support the idea that
450 MADS transcription factors collaborate with the SAS complex to regulate the
451 transcription of genes involved in flower development.

452 **The accessibility generated by SAS in inflorescence is required for AP1 binding**

453 We chose AP1, one famous MADS transcription factor crucial for floral identity, as an
454 example to study the relationship between MADS transcription factors and SAS in
455 inflorescences. At the genomic regions showing down-regulated accessibility in the
456 SAS mutants, the ATAC-seq signals in the *ap1* mutant are overall not affected compared
457 to the wild-type plants in inflorescences (Fig. 7A). There are few differential accessible
458 regions in *ap1* compared with the wild-type plants in inflorescences (Fig. 7B). These
459 data indicate that AP1 is unlikely to function upstream to the SAS complex.

460 We therefore investigated whether AP1 functions downstream of SAS by performing
461 ChIP-seq of AP1 in the inflorescences of wild-type and *syd* mutant plants. The ChIP-
462 seq data indicated that the average enrichment of AP1 is markedly decreased in *syd*
463 compared to the wild type (Fig. 7C), suggesting that the genomic binding of AP1 is
464 partially dependent on SAS. By overlapping the AP1-binding regions and the regions
465 showing down-regulated accessibility in the *syd* mutant, we found most of the
466 accessible regions regulated by SAS in inflorescences are bound by AP1 (Fig. 7D).
467 Among the binding regions of AP1, the regions with down-regulated accessibility in
468 *syd* show a significant higher AP1 enrichment than the regions with maintained
469 accessibility (Fig. 7E), and the enrichment of AP1 in SAS-regulated accessible regions
470 is significantly decreased in the *syd* mutant compared to the wild type (Fig. 7E). The
471 effects of *syd* on chromatin accessibility and the genomic binding of AP1 were
472 exemplified by the screenshot of a representative genomic region (Fig. 7F). In addition,
473 *AP3* (Hill et al., 1998) and *ZP1* (Hu et al., 2023), two well-known target genes of AP1,

474 show consistent decrease of chromatin accessibility and AP1 enrichment in the *syd*
475 mutant relative to the wild type (Fig.7G). These data suggest that the SAS-dependent
476 chromatin accessibility contributes to the binding of AP1 to its target genomic loci.

477

478 **Discussion**

479 SWI/SNF complexes play crucial roles in the regulation of diverse developmental
480 processes in both metazoans and plants. Recent studies have illustrated the functional
481 variations among the three Arabidopsis SWI/SNF complexes: BAS, SAS, and MAS
482 (Guo et al., 2022; Fu et al., 2023). However, the precise mechanisms by which these
483 complexes exert specific functions during different developmental stages remain
484 largely unknown. In this study, we performed a comprehensive analysis to compare the
485 impact of BAS, SAS, and MAS on chromatin accessibility throughout the entire
486 genome between vegetative and reproductive development processes. Our results
487 demonstrate that while the three SWI/SNF complexes contribute to a comparable
488 amount of accessible regions in seedlings, there is a significantly higher proportion of
489 inflorescence-specific accessible regions that depend on SAS. This indicates that SAS
490 exhibits a stronger influence on inflorescences compared to BAS and MAS. The
491 findings highlight the specific role of SAS in inflorescences, which is consistent with
492 the more severe defects in floral development observed in SAS mutants relative to BAS
493 and MAS mutants.

494 Our analysis, combining ATAC-seq with ChIP-seq data, implicates two mechanisms
495 through which the SAS complex contributes to establishing the accessibility of genes
496 involved in flower development. Firstly, SAS is recruited to genes involved in flower
497 development, thereby establishing the accessibility of these genes. It is likely that
498 multiple transcription factors collaborate to recruit SAS to different sets of flower
499 development related genes. Secondly, the SAS complex exhibits constant binding to
500 genes involved in flower development during both the vegetative and reproductive

processes, with an enhanced chromatin remodeling activity specifically during the reproductive process. The change in the chromatin remodeling activity of SAS at different developmental stages can be attributed to either its differential recognition ability to histone modifications or its interactions with different transcription factors. Further studies are needed to investigate how histone modifications and/or transcription factors regulate the recruitment of SAS to chromatin or its chromatin remodeling activity during the reproductive process.

A previous study have indicated that establishing the accessibility of distal accessible regions is critical for the activation of genes involved in flower development during reproductive development (Yan et al., 2019). However, the specific mechanisms responsible for establishing accessibility in the distal regions during the reproductive process remain largely unclear. Our findings show that the SAS complex is recruited to numerous genes involved in flower development during the reproductive process and plays a crucial role in establishing their accessibility. While BAS and SAS target similar genomic regions, SAS exhibits a greater ability to regulate the accessibility of distal accessible regions. This suggests that the impact of SAS on chromatin accessibility is not only regulated by its binding to chromatin but also by its chromatin remodeling activity. Notably, distal accessible regions generally exhibit lower levels of histone acetylation compared to proximal promoter regions (Yan et al., 2019), indicating that differential histone modifications may regulate the remodeling activities of BAS and SAS. These findings are consistent with studies conducted in mammals, which have demonstrated the impact of histone modifications on the genomic targeting and remodeling activity of various SWI/SNF complexes (Mashtalir et al., 2021). In contrast to SAS and BAS, MAS primarily contributes to the accessibility of genes unrelated to flower development (such as housekeeping genes), further highlighting the functional specificities of different SWI/SNF complexes in Arabidopsis.

In mammals, there are three classes of SWI/SNF complexes: BAF, PBAF, and ncBAF. Among these, the BAF complex has been shown to specifically target distal enhancer

529 regions, which play a crucial role in facilitating the transcription of genes involved in
530 development (Alver et al., 2017). Similarly, in Arabidopsis, distal accessible regions
531 have been identified as predictive markers for intergenic enhancers, exhibiting highly
532 stage-specific patterns during flower development (Zhu et al., 2015; Yan et al., 2019).
533 In this study, we present evidence that the SAS complex specifically contributes to the
534 accessibility of distal accessible regions for numerous genes involved in flower
535 development. This suggests that the SAS complex serves as the primary chromatin
536 remodeler responsible for establishing the stage-specific accessibility of genes involved
537 in flower development. Thus, it is likely that the SAS complex functions as the
538 counterpart of the human BAF complex in regulating the accessibility of distal enhancer
539 regions in genes related to flower development.

540 Transcription factors are known to have cell-type-specific functions, while chromatin
541 remodeling complexes are generally considered to have broader regulatory roles. It is
542 likely that the SAS complex collaborates with transcription factors to regulate gene
543 transcription during reproductive development. Transcription factors can either bind the
544 accessible cis-regulatory regions generated by chromatin remodelers or function as the
545 pioneer transcription factors to bind the nucleosome DNA and recruitment the
546 chromatin remodelers to generate accessibility. In Arabidopsis, LFY has been identified
547 as a pioneer transcription factor that binds to nucleosome DNA and recruit SWI/SNF
548 components to establish the accessibility of genes responsible for determining the floral
549 organ identity (Jin et al., 2021; Lai et al., 2021). Certain MADS transcription factors,
550 such as AP1 and SEP3, have also been suggested as potential pioneer factors involved
551 in flower development (Lai et al., 2018). However, our results suggest that AP1 is not
552 likely to be a pioneer transcription factor. Oppositely, the chromatin accessibility
553 generated by SAS is crucial for the binding of AP1, indicating that AP1 functions
554 downstream of chromatin accessibility. Interestingly, we found most of the accessible
555 regions generated by SAS in inflorescences are occupied by AP1 with high enrichment,
556 indicating that the chromatin remodeling of SAS is highly correlated with the flower
557 development regulation of AP1 in inflorescences. This result is consistent with our

558 motif analysis that MADS TF motifs are significantly enriched in the inflorescence-
559 specific binding regions of SAS.

560 In mammals, the abundance of chromatin remodelers compared to transcription factors
561 has facilitated the identification of chromatin remodelers co-purified with transcription
562 factors. However, the identification of transcription factors co-purified with chromatin
563 remodelers has proven challenging (Gourisankar et al., 2023). Similar difficulties have
564 been encountered in plants, where MADS transcription factors have been used as baits
565 to successfully identify SWI/SNF components, while attempts to identify MADS
566 transcription factors using SWI/SNF components as baits have been unsuccessful
567 (Smaczniak et al., 2012; Guo et al., 2022). In a recent online study, the interaction
568 between transcription factors and components of chromatin-remodeling complexes
569 during stomatal development was identified using proximity labeling methods (Liu et
570 al., 2023). In the future, investigating the specific interaction between SWI/SNF
571 chromatin complexes and different transcription factors during flower development will
572 contribute to our understanding of the molecular mechanisms underlying the specific
573 functions of the SAS complex in flower development.

574 **Materials and methods**

575 **Plant materials**

576 Arabidopsis were in the Columbia-0 (Col-0) ecotype. SWI/SNF mutants related to this
577 study include: *brm-1* (SALK_030046C), *syd* (CS822017), *swi3d* (SALK_100310),
578 *minu1* (SALK_015562), *minu2* (SALK_057856), *pms2a* (SALK_141512), *pms2b*
579 (SALK_010411), and *sys1/2/3* (generated by CRISPR-Cas9 system), *ap1*
580 (SALK_151561）. Double mutants are generated by crossing. Detailed information on
581 genotyping primers and CRISPR-Cas9 targets for SWI/SNF mutants can be found in
582 the previous study (Guo et al., 2022). Full length genomic sequences of genes driven
583 by 1.5-2 kb native promoter were cloned into modified pCAMBIA-1305-GFP or
584 pCAMBIA-1305-3×Flag to generate C-terminal tagged transgenes for ChIP-seq. The

585 primers used for these constructions can be found in the previous study (Guo et al.,
586 2022). Arabidopsis seeds were sown on the Murahsige and Skoog (MS) medium and
587 stratified at 4 ℃ for 2 days. Subsequently, they were grown under long-day conditions
588 (16 h of light at 23 ℃ and 8 h of darkness at 22 ℃). Whole plants of 12-day-old
589 seedlings grown on MS medium and inflorescences of 4~5-week-old plants in soil were
590 used for RNA-seq, ATAC-seq, and ChIP-seq experiments.

591 **RNA-seq and data analysis**

592 About 0.1 gram of the inflorescence tips from the SWI/SNF mutants and the wild-type
593 plants were harvested and ground in liquid nitrogen. For each genotype, three
594 independent samples were collected as biological replicates. RNA was isolated by
595 TRIzol reagent (Invitrogen, 15596018). Library construction and sequencing were
596 carried out by BGI (Wuhan, China) using the DNBSEQ platform (sequencing method:
597 SE50). The raw reads of RNA-seq were processed with the removal of adaptor
598 sequences and the filter of low-quality reads. The clean reads were then mapped to the
599 Arabidopsis genome using HISAT2 (version 2.2.1) (Kim et al., 2015) with default
600 parameters. After counting the reads mapped on the exon by featureCounts (version
601 2.0.1)(Liao et al., 2014), edgeR (version 3.32.1) (Robinson et al., 2010) was used to
602 evaluate the expression level, fold change and False Discovery Rate (FDR) of each
603 gene. DEGs were filtered based on the criteria of $|\log2FC| \geq 1$ and $FDR < 0.05$.

604 **ATAC-seq and data analysis**

605 About 0.1-0.2 gram of the inflorescence tips from the SWI/SNF mutants and the wild-
606 type plants were used for ATAC-seq. Two biological replicates were set for each
607 genotype. The ATAC-seq experiments were performed according to the previous study
608 (Guo et al., 2022). After extracting and assessing the quality of the nuclei, about
609 10000~50000 nuclei of each sample were collected for Tn5 tagmentation-based library
610 construction using TruePrep DNA library Prep Kit V2 for Illumina (Vazyme, TD501).
611 The ATAC-seq libraries were sent to Novogene and sequenced by an Illumina-NovaSeq

612 6000 (sequencing method: PE150).

613 The raw data were processed with Trim Galore (version 0.6.6) (Krueger, 2015) to
614 remove adaptors and low-quality reads. Clean reads were then mapped to the
615 Arabidopsis genome using bowtie2 (version 2.4.2) (Langmead and Salzberg, 2012)
616 with the multi-mapped reads or PCR duplicates filtered out. The unique mapped reads
617 were converted to bigwig files by bamCoverage in Deeptools (version 3.5.1)(Ramírez
618 et al., 2016) with the parameter 'binSize 10' and 'normalizeUsing RPKM' and then
619 visualized by the Integrative Genomics Viewer (IGV) (version 2.4.13) for snapshots.
620 Accessible peaks were called using macs2 (version 2.2.7.1) (Zhang et al., 2008) with
621 the following parameter: macs2 callpeak -t sample.bam -f BAMPE -g 1.2e+8 -nomodel
622 --bdg --keep-dup all. Only the peaks that present in both replicates (irreproducible
623 discovery rate < = 0.05) were retained for further analysis. Differentially accessible
624 regions between the two samples were identified using the method 'DESEQ2' in
625 DiffBind (version 3.0.15) (Rossinnes et al., 2011), with criteria of |log2FC| ≥0.5 and
626 FDR < 0.05. Peaks were assigned to genes with the same rules as described in the
627 previous study (Guo et al., 2022). Briefly, a peak that overlapped with the gene body
628 including 1 kb upstream region were annotated to the corresponding gene, and if a peak
629 was overlapped with more than one gene, it was annotated to the gene harboring the
630 closest TSS to the midpoint of the peak.

631 **GSEA and GO analyses**

632 The GSEA analysis was performed based on the gene sets generated from ATAC-seq
633 analysis in this study and the RNA-seq data of various Arabidopsis tissues from the
634 published study (Mergner et al., 2020). The expression level in flower and the average
635 expression level across different tissues of the total Arabidopsis genes were used as the
636 input expression dataset and the GSEA analysis was performed using GSEA software
637 (version 4.3.2) according to the manual (Subramanian et al., 2005). The parameter
638 'Metric for ranking genes' was set as 'Diff_of_Classes'. The term 'flower specificity'
639 represents the expression level of a gene in the flower minus the average expression

level of that gene across all the tissues. The GO analysis was performed by ClusterProfiler (version 4.2.2) (Yu et al., 2012) using the 'org.At.tair.db' database.

ChIP-seq and data analysis

ChIP-seq were performed following the protocol from the previous studies with minor changes (Gendrel et al., 2005; Guo et al., 2022). Briefly, 4 grams of fresh seedlings or the inflorescence tips were collected and cross-linked in the buffer containing 1% formaldehyde under vacuum. The nuclei were extracted, washed, and sonicated by the Bioruptor 2000 in the sonication buffer containing 0.33% SDS. Subsequently, the fragmented chromatin was separated by centrifugation and the SDS concentration was diluted to 0.1%. For each sample, 0.1% of the total volume was set aside as the input sample, while the remaining diluted chromatin fragments were incubated overnight with the GFP antibody (Abcam, ab290) at a 1:600 dilution. The Dynabeads Protein A (Invitrogen, 100.01D) were added into the solution and incubated for 2-3 h, and then washed sequentially with low-salt buffer, high-salt buffer, and LiCl buffer, followed by two washes with TE buffer. The DNA-protein complexes were then eluted from the beads and de-crosslinked at 65°C overnight. After the digestion of RNA and protein, the DNA was purified for library construction using NEBnext® Ultra™ II DNA Library Prep Kit for Illumina (E7654S). The ChIP-seq libraries were sent to Novogene (Tianjin, China) for sequencing using an Illumina-NovaSeq 6000 (sequencing method: PE150).

After removal of adaptors from the raw reads, the clean reads were mapped to the Arabidopsis genome using Bowtie2 (version 2.4.2) with the same mapping method as for the ATAC-seq data. The binding peaks were called by macs2 (version 2.2.7.1) with the following parameters: macs2 callpeak -c input.bam -t IP.bam -f BAMPE -g 1.2e+8. Peaks were filtered and visualized using the same methods and standards as described in the ATAC-seq data analysis. Differential binding peaks of SWI/SNF subunits between seedlings and inflorescences were identified using the 'DESEQ2' method in DiffBind (version 3.0.15), with criteria of $|\log2FC| \geq 0.5$ and $FDR < 0.05$. The TF motif analysis was conducted by the findMotifsGenome.pl program in Homer (version

668 4.11)(Heinz et al., 2010) with default parameters using different sets of regions as input
669 files.

670 **Plotting methods**

671 The MDS plot were generated using the plotMDS function of the R package edgeR
672 (version 3.32.1) with default parameters. The scatter plot was created using the
673 ggscatter function of the R package ggpubr (version 0.4.0)(Kassambara, 2020). The
674 PCA plot were generated using DiffBind (version 3.0.15) with default parameters. The
675 heatmap based on Pearson correlation coefficients was generated using the heatmap.2
676 function of the R package gplots (version 3.1.1)(Warnes et al., 2014). Bar charts and
677 the pie chart were created using Graphpad Prism (version 8.0). Box plots were
678 generated using the boxplot function in R (version 4.1.0). The heatmap representing the
679 enrichment of TF motifs was generated using Pheatmap (version 1.0.12) (Kolde, 2012).
680 Venn diagrams, butterfly bar plots, the volcano plot, and the bubble plot containing
681 multiple GO results of different samples were created using an online platform for data
682 analysis and visualization at https://www.bioinfomatics.com.cn. The bubble plot
683 showing the overlap of TF binding regions and the SAS-specific binding regions were
684 plotted using ggplot2 (version 3.3.6).

685 **Accession numbers**

686 The accession numbers of genes reported in this study are as follows: AT2G46020
687 (*BRM*), AT2G28290 (*SYD*), AT4G34430 (*SWI3D*), AT5G07940 (*SYS1*), AT5G07970
688 (*SYS2*), AT5G07980 (*SYS3*), AT3G06010 (*MINU1*), AT5G19310 (*MINU2*),
689 AT3G08020 (*PMS2A*), AT3G52100 (*PMS2B*) and AT1G69120 (*AP1*).

690 **Data availability**

691 The raw data for ATAC-seq, ChIP-seq, and RNA-seq experiments have been deposited
692 in the Gene Expression Omnibus (GEO) database under the accession numbers
693 GSE254654, GSE254655, and GSE254656, respectively. The access tokens are as

694 follows: inapmusabpcvvar for GSE254654, wbahscwojrotpqn for GSE254655, and
695 kfqbwguylhudhmh for GSE254656.

696 **Author contribution**

697 JG and XJH conceived the project and designed the experiments. JG and ZZL
698 performed the experiments. JG and YNS performed the bioinformatic analysis. JG and
699 XJH wrote the manuscript.

700 **Acknowledgements**

701 This work was supported by the National Natural Science Foundation of China to X. J.
702 He (32025003).

703 **References**

704 **Alver, B.H., Kim, K.H., Lu, P., Wang, X., Manchester, H.E., Wang, W., Haswell,**
705 **J.R., Park, P.J., and Roberts, C.W.** (2017). The SWI/SNF chromatin
706 remodelling complex is required for maintenance of lineage specific enhancers.
707 Nat Commun **8**, 1-10.

708 **Archacki, R., Sarnowski, T.J., Halibart-Puzio, J., Brzeska, K., Buszewicz, D.,**
709 **Prymakowska-Bosak, M., Koncz, C., and Jerzmanowski, A.** (2009). Genetic
710 analysis of functional redundancy of BRM ATPase and ATSWI3C subunits of
711 Arabidopsis SWI/SNF chromatin remodelling complexes. Planta **229,** 1281-
712 1292.

713 **Bezhani, S., Winter, C., Hershman, S., Wagner, J.D., Kennedy, J.F., Kwon, C.S.,**
714 **Pfluger, J., Su, Y., and Wagner, D.** (2007). Unique, shared, and redundant roles
715 for the Arabidopsis SWI/SNF chromatin remodeling ATPases BRAHMA and
716 SPLAYED. Plant Cell **19,** 403-416.

717 **Bieluszewski, T., Prakash, S., Roulé, T., and Wagner, D.** (2023). The Role and
718 Activity of SWI/SNF Chromatin Remodelers. Annu Rev Plant Biol **74,** 139-163.

719 **Cairns, B.R., Kim, Y.-J., Sayre, M.H., Laurent, B.C., and Kornberg, R.D.** (1994).

720 A multisubunit complex containing the SWI1/ADR6, SWI2/SNF2, SWI3,
721 SNF5, and SNF6 gene products isolated from yeast. Proc Natl Acad Sci U S A
722 **91,** 1950-1954.
723 **Cenik, B.K., and Shilatifard, A.** (2020). COMPASS and SWI/SNF complexes in
724 development and disease. Nat Rev Genet **22**, 38-58.
725 **Chen, D., Yan, W., Fu, L.Y., and Kaufmann, K.** (2018). Architecture of gene
726 regulatory networks controlling flower development in *Arabidopsis thaliana*.
727 Nat Commun **9,** 4534.
728 **Chen, X., Zhang, Z., Liu, D., Zhang, K., Li, A., and Mao, L.** (2010). SQUAMOSA
729 promoter-binding protein-like transcription factors: star players for plant growth
730 and development. J Integr Plant Biol **52,** 946-951.
731 **Cheng, C.Y., Krishnakumar, V., Chan, A.P., Thibaud-Nissen, F., Schobel, S., and**
732 **Town, C.D.** (2017). Araport11: a complete reannotation of the *Arabidopsis*
733 *thaliana* reference genome. Plant J **89,** 789-804.
734 **Clapier, C.R., Iwasa, J., Cairns, B.R., and Peterson, C.L.** (2017). Mechanisms of
735 action and regulation of ATP-dependent chromatin-remodelling complexes. Nat
736 Rev Mol Cell Biol **18,** 407-422.
737 **Diego-Martin, B., Pérez-Alemany, J., Candela-Ferre, J., Corbalán-Acedo, A.,**
738 **Pereyra, J., Alabadí, D., Jami-Alahmadi, Y., Wohlschlegel, J., and Gallego-**
739 **Bartolomé, J.** (2022). The TRIPLE PHD FINGERS proteins are required for
740 SWI/SNF complex-mediated +1 nucleosome positioning and transcription start
741 site determination in Arabidopsis. Nucleic Acids Res **50,** 10399-10417.
742 **Ditta, G., Pinyopich, A., Robles, P., Pelaz, S., and Yanofsky, M.F.** (2004). The *SEP4*
743 gene of *Arabidopsis thaliana* functions in floral organ and meristem identity.
744 Curr Biol **14,** 1935-1940.
745 **Farrona, S., Hurtado, L., Bowman, J.L., and Reyes, J.C.** (2004). The *Arabidopsis*
746 *thaliana* SNF2 homolog AtBRM controls shoot development and flowering.
747 Development **131,** 4965-4975.
748 **Fu, W., Yu, Y., Shu, J., Yu, Z., Zhong, Y., Zhu, T., Zhang, Z., Liang, Z., Cui, Y.,**
749 **Chen, C., et al.** (2023). Organization, genomic targeting, and assembly of three

750 distinct SWI/SNF chromatin remodeling complexes in Arabidopsis. Plant Cell
751 **35,** 2464-2483.
752 **Gendrel, A.-V., Lippman, Z., Martienssen, R., and Colot, V.** (2005). Profiling
753 histone modification patterns in plants using genomic tiling microarrays. Nat
754 Methods **2,** 213-218.
755 **Gourisankar, S., Krokhotin, A., Wenderski, W., and Crabtree, G.R.** (2023).
756 Context-specific functions of chromatin remodellers in development and
757 disease. Nat Rev Genet Published online November 24, 2023. doi:
758 10.1038/s41576-023-00666-x
759 **Guo, J., Cai, G., Li, Y.Q., Zhang, Y.X., Su, Y.N., Yuan, D.Y., Zhang, Z.C., Liu, Z.Z.,**
760 **Cai, X.W., Guo, J., et al.** (2022). Comprehensive characterization of three
761 classes of Arabidopsis SWI/SNF chromatin remodelling complexes. Nat Plants
762 **8,** 1423-1439.
763 **Heinz, S., Benner, C., Spann, N., Bertolino, E., Lin, Y.C., Laslo, P., Cheng, J.X.,**
764 **Murre, C., Singh, H., and Glass, C.K.** (2010). Simple combinations of
765 lineage-determining transcription factors prime cis-regulatory elements
766 required for macrophage and B cell identities. Mol Cell **38,** 576-589.
767 **Hill, T.A., Day, C.D., Zondlo, S.C., Thackeray, A.G., and Irish, V.F.** (1998). Discrete
768 spatial and temporal cis-acting elements regulate transcription of the
769 Arabidopsis floral homeotic gene *APETALA3*. Development **125,** 1711-1721.
770 **Ho, L., and Crabtree, G.R.** (2010). Chromatin remodelling during development.
771 Nature **463,** 474-484.
772 **Hu, T., Li, X., Du, L., Manuela, D., and Xu, M.** (2023). LEAFY and APETALA1
773 down-regulate ZINC FINGER PROTEIN 1 and 8 to release their repression on
774 class B and C floral homeotic genes. Proc Natl Acad Sci U S A **120,**
775 e2221181120.
776 **Hurtado, L., Farrona, S., and Reyes, J.C.** (2006). The putative SWI/SNF complex
777 subunit BRAHMA activates flower homeotic genes in *Arabidopsis thaliana*.
778 Plant Mol Biol **62,** 291-304.
779 **Jaronczyk, K., Sosnowska, K., Zaborowski, A., Pupel, P., Bucholc, M., Malecka,**

E., Siwirykow, N., Stachula, P., Iwanicka-Nowicka, R., and Koblowska, M. (2021). Bromodomain-containing subunits BRD1, BRD2, and BRD13 are required for proper functioning of SWI/SNF complexes in Arabidopsis. Plant Commun **2,** 100174.

Jin, R., Klasfeld, S., Zhu, Y., Garcia, M.F., Xiao, J., Han, S.-K., Konkol, A., and Wagner, D. (2021). LEAFY is a pioneer transcription factor and licenses cell reprogramming to floral fate. Nat Commun **12,** 1-14.

Kassambara, A. (2020). ggpubr:'ggplot2'based publication ready plots. R package version 0.4. 0.

Kennison, J.A., and Tamkun, J.W. (1988). Dosage-dependent modifiers of polycomb and antennapedia mutations in Drosophila. Proc Natl Acad Sci U S A **85,** 8136-8140.

Kim, D., Langmead, B., and Salzberg, S.L. (2015). HISAT: a fast spliced aligner with low memory requirements. Nat Methods **12,** 357-360.

Kolde, R. (2012). Pheatmap: pretty heatmaps. R package version **1**.

Krueger, F. (2015). Trim galore. A wrapper tool around Cutadapt and FastQC to consistently apply quality and adapter trimming to FastQ files **516**.

Kwon, C.S., Chen, C.B., and Wagner, D. (2005). *WUSCHEL* is a primary target for transcriptional regulation by SPLAYED in dynamic control of stem cell fate in Arabidopsis. Genes Dev **19,** 992-1003.

Lai, X., Verhage, L., Hugouvieux, V., and Zubieta, C. (2018). Pioneer Factors in Animals and Plants-Colonizing Chromatin for Gene Regulation. Molecules **23,** 1914.

Lai, X., Blanc-Mathieu, R., GrandVuillemin, L., Huang, Y., Stigliani, A., Lucas, J., Thévenon, E., Loue-Manifel, J., Turchi, L., Daher, H., et al. (2021). The LEAFY floral regulator displays pioneer transcription factor properties. Mol Plant **14,** 829-837.

Langmead, B., and Salzberg, S.L. (2012). Fast gapped-read alignment with Bowtie 2. Nat Methods **9,** 357.

Li, C., Chen, C., Gao, L., Yang, S., Vi, N., Shi, X., Siminovitch, K., Kohalmi, S.E.,

Huang, S., Wu, K., et al. (2015). The Arabidopsis SWI2/SNF2 Chromatin Remodeler BRAHMA Regulates Polycomb Function during Vegetative Development and Directly Activates the Flowering Repressor Gene *SVP*. Plos Genet **11,** e1004944.

Li, C., Gu, L., Gao, L., Chen, C., Wei, C.-Q., Qiu, Q., Chien, C.-W., Wang, S., Jiang, L., Ai, L.-F., et al. (2016). Concerted genomic targeting of H3K27 demethylase REF6 and chromatin-remodeling ATPase BRM in Arabidopsis. Nat Genet **48,** 687-693.

Liao, Y., Smyth, G.K., and Shi, W. (2014). featureCounts: an efficient general purpose program for assigning sequence reads to genomic features. Bioinformatics **30,** 923-930.

Lin, X., Yuan, T., Guo, H., Guo, Y., Yamaguchi, N., Wang, S., Zhang, D., Qi, D., Li, J., Chen, Q., et al. (2023). The regulation of chromatin configuration at *AGAMOUS* locus by LFR-SYD-containing complex is critical for reproductive organ development in Arabidopsis. Plant J **116,** 478-496.

Liu, A., Mair, A., Matos, J.L., Vollbrecht, M., Xu, S.L., and Bergmann, D.C. (2023). Cell Fate Programming by Transcription Factors and Epigenetic Machinery in Stomatal Development. bioRxiv. doi:10.1101/2023.08.23.554515

Mashtalir, N., Dao, H.T., Sankar, A., Liu, H., Corin, A.J., Bagert, J.D., Ge, E.J., D'Avino, A.R., Filipovski, M., and Michel, B.C. et al. (2021). Chromatin landscape signals differentially dictate the activities of mSWI/SNF family complexes. Science **373,** 306-315.

Mergner, J., Frejno, M., List, M., Papacek, M., Chen, X., Chaudhary, A., Samaras, P., Richter, S., Shikata, H., Messerer, M., et al. (2020). Mass-spectrometry-based draft of the Arabidopsis proteome. Nature **579,** 409-414.

Pelaz, S., Ditta, G.S., Baumann, E., Wisman, E., and Yanofsky, M.F. (2000). B and C floral organ identity functions require *SEPALLATA* MADS-box genes. Nature **405,** 200-203.

Peterson, C.L., Dingwall, A., and Scott, M.P. (1994). Five SWI/SNF gene products are components of a large multisubunit complex required for transcriptional

840 enhancement. Proc Natl Acad Sci U S A **91,** 2905-2908.
841 **Ramírez, F., Ryan, D.P., Grüning, B., Bhardwaj, V., Kilpert, F., Richter, A.S.,**
842 **Heyne, S., Dündar, F., and Manke, T.** (2016). deepTools2: a next generation
843 web server for deep-sequencing data analysis. Nucleic Acids Res **44,** W160-
844 W165.
845 **Robinson, M.D., McCarthy, D.J., and Smyth, G.K.** (2010). edgeR: a Bioconductor
846 package for differential expression analysis of digital gene expression data.
847 Bioinformatics **26,** 139-140.
848 **Rossinnes, C.S., Stark, R., Teschendorff, A.E., Holmes, K.A., Ali, H.R., Dunning,**
849 **M.J., Brown, G.D., Gojis, O., Ellis, I.O., and Green, A.R.** (2011). Differential
850 oestrogen receptor binding is associated with clinical outcome in breast cancer.
851 Nature **481,** 389-393.
852 **Sang, Y., Silva-Ortega, C.O., Wu, S., Yamaguchi, N., Wu, M.-F., Pfluger, J.,**
853 **Gillmor, C.S., Gallagher, K.L., and Wagner, D.** (2012). Mutations in two non-
854 canonical Arabidopsis SWI2/SNF2 chromatin remodeling ATPases cause
855 embryogenesis and stem cell maintenance defects. Plant J **72,** 1000-1014.
856 **Sarnowski, T.J., Rios, G., Jasik, J., Swiezewski, S., Kaczanowski, S., Li, Y.,**
857 **Kwiatkowska, A., Pawlikowska, K., Kozbial, M., Kozbial, P., et al.** (2005).
858 SWI3 subunits of putative SWI/SNF chromatin-remodeling complexes play
859 distinct roles during Arabidopsis development. Plant Cell **17,** 2454-2472.
860 **Schultz, E.A., and Haughn, G.W.** (1991). *LEAFY*, a Homeotic Gene That Regulates
861 Inflorescence Development in Arabidopsis. Plant Cell **3,** 771-781.
862 **Shu, J., Chen, C., Li, C., Thapa, R.K., Song, J., Xie, X., Nguyen, V., Bian, S., Liu,**
863 **J., and Kohalmi, S.E.** (2021). Genome-wide occupancy of Arabidopsis
864 SWI/SNF chromatin remodeler SPLAYED provides insights into its interplay
865 with its close homolog BRAHMA and Polycomb proteins. Plant J **106,** 200-213.
866 **Smaczniak, C., Immink, R.G., Muiño, J.M., Blanvillain, R., Busscher, M.,**
867 **Busscher-Lange, J., Dinh, Q.D., Liu, S., Westphal, A.H., Boeren, S., et al.**
868 (2012). Characterization of MADS-domain transcription factor complexes in
869 Arabidopsis flower development. Proc Natl Acad Sci U S A **109,** 1560-1565.

870 **Stortenbeker, N., and Bemer, M.** (2019). The *SAUR* gene family: the plant's toolbox
871 for adaptation of growth and development. J Exp Bot **70,** 17-27.
872 **Subramanian, A., Tamayo, P., Mootha, V.K., Mukherjee, S., Ebert, B.L., Gillette,**
873 **M.A., Paulovich, A., Pomeroy, S.L., Golub, T.R., Lander, E.S., and Mesirov,**
874 **J.P.** (2005). Gene set enrichment analysis: a knowledge-based approach for
875 interpreting genome-wide expression profiles. Proc Natl Acad Sci U S A **102,**
876 15545-15550.
877 **Tamkun, J.W., Deuring, R., Scott, M.P., Kissinger, M., Pattatucci, A.M., Kaufman,**
878 **T.C., and Kennison, J.A.** (1992). brahma: a regulator of Drosophila homeotic
879 genes structurally related to the yeast transcriptional activator SNF2/SWI2. Cell
880 **68,** 561-572.
881 **Theißen, G., Melzer, R., and Rümpler, F.** (2016). MADS-domain transcription factors
882 and the floral quartet model of flower development: linking plant development
883 and evolution. Development. **143,** 3259-3271.
884 **van Mourik, H., Chen, P., Smaczniak, C., Boeren, S., Kaufmann, K., Bemer, M.,**
885 **Angenent, G.C., and Muino, J.M.** (2023). Dual specificity and target gene
886 selection by the MADS-domain protein FRUITFULL. Nat Plants **9,** 473-485.
887 **Wagner, D., and Meyerowitz, E.M.** (2002). SPLAYED, a novel SWI/SNF ATPase
888 homolog, controls reproductive development in Arabidopsis. Curr Biol **12,** 85-
889 94.
890 **Warnes, G.R., Bolker, B., Bonebakker, L., Gentleman, R., Liaw, W.H.A., Lumley,**
891 **T., Maechler, M., Magnusson, A., Moeller, S., and Schwartz, M.** (2014).
892 Gplots: various R programming tools for plotting data. 2016. R package version
893 **2**.
894 **Weigel, D.** (1995). The genetics of flower development: from floral induction to ovule
895 morphogenesis. Annu Rev Genet **29,** 19-39.
896 **Wu, M.-F., Yamaguchi, N., Xiao, J., Bargmann, B., Estelle, M., Sang, Y., and**
897 **Wagner, D.** (2015). Auxin-regulated chromatin switch directs acquisition of
898 flower primordium founder fate. elife **4,** e09269.
899 **Wu, M.-F., Sang, Y., Bezhani, S., Yamaguchi, N., Han, S.-K., Li, Z., Su, Y.,**

900 **Slewinski, T.L., and Wagner, D.** (2012). SWI2/SNF2 chromatin remodeling
901 ATPases overcome polycomb repression and control floral organ identity with
902 the LEAFY and SEPALLATA3 transcription factors. Proc Natl Acad Sci U S A
903 **109,** 3576-3581.
904 **Yan, W., Chen, D., Schumacher, J., Durantini, D., Engelhorn, J., Chen, M., Carles,**
905 **C.C., and Kaufmann, K.** (2019). Dynamic control of enhancer activity drives
906 stage-specific gene expression during flower morphogenesis. Nature Commun
907 **10,** 1-16.
908 **Yu, G., Wang, L.G., Han, Y., and He, Q.Y.** (2012). clusterProfiler: an R package for
909 comparing biological themes among gene clusters. Omics **16,** 284-287.
910 **Yu, Y., Liang, Z., Song, X., Fu, W., Xu, J., Lei, Y., Yuan, L., Ruan, J., Chen, C., and**
911 **Fu, W.** (2020). BRAHMA-interacting proteins BRIP1 and BRIP2 are core
912 subunits of Arabidopsis SWI/SNF complexes. Nature Plants **6,** 1-12.
913 **Yu, Y., Fu, W., Xu, J., Lei, Y., Song, X., Liang, Z., Zhu, T., Liang, Y., Hao, Y., and**
914 **Yuan, L. et al.** (2021). Bromodomain-containing proteins BRD1, BRD2, and
915 BRD13 are core subunits of SWI/SNF complexes and vital for their genomic
916 targeting in Arabidopsis. Mol Plant **14**, 888-904
917 **Zhang, Y., Liu, T., Meyer, C.A., Eeckhoute, J., Johnson, D.S., Bernstein, B.E.,**
918 **Nusbaum, C., Myers, R.M., Brown, M., and Li, W.** (2008). Model-based
919 analysis of ChIP-Seq (MACS). Genome Biol **9,** R137.
920 **Zhao, H., Yang, M., Bishop, J., Teng, Y., Cao, Y., Beall, B.D., Li, S., Liu, T., Fang,**
921 **Q., Fang, C., et al.** (2022). Identification and functional validation of super-
922 enhancers in Arabidopsis thaliana. Proc Natl Acad Sci U S A **119,** e2215328119.
923 **Zhu, B., Zhang, W., Zhang, T., Liu, B., and Jiang, J.** (2015). Genome-Wide
924 Prediction and Validation of Intergenic Enhancers in Arabidopsis Using Open
925 Chromatin Signatures. Plant Cell **27,** 2415-2426.
926
927

928 **Figure legends**

929 **Figure 1.** Comparison of DEGs identified by RNA-seq in SWI/SNF mutants between
930 inflorescences and seedlings. **A)** MDS plot of the inflorescence RNA-seq samples.
931 Clustering of BAS, SAS and MAS mutants are marked with green, blue, and red circles,
932 respectively. **B)** Heat map showing the pairwise Pearson correlation coefficients based
933 on the expression fold changes in inflorescences for the total DEGs of the displayed
934 SWI/SNF mutants. **C)** The number of DEGs in SWI/SNF mutants relative to the wild
935 type in both seedlings and inflorescences. **D)** The scatter plot showing the correlation
936 between the average petal number (Guo et al., 2022) and the number of DEGs in
937 inflorescences of the SWI/SNF mutants. A fitted regression line and a 95% confidence
938 interval band are indicated. R represents the Pearson correlation coefficient. *P* value
939 was determined by two-tailed *t* test. **E-G)** The overlap of up-regulated genes and down-
940 regulated DEGs in seedlings and inflorescences of *brm* (**E**), *syd* (**F**) and *minu1/2* (**G**).
941 The purple bars below the venn diagram marked with 'a' and 'b' represent genes shared
942 by other sets and genes specifically belonging to one set of the venn diagrams,
943 respectively.

944 **Figure 2.** Analysis of differentially accessible regions in inflorescences of SWI/SNF
945 mutants relative to the wild type. **A)** Principal component analysis **(**PCA) of the
946 inflorescence ATAC-seq data of the wild type and SWI/SNF mutants. The cluster of
947 SAS mutants are marked with the blue circle. **B)** The number of up-regulated and down-
948 regulated differentially accessible regions in inflorescences of the SWI/SNF mutants
949 identified by ATAC-seq. The number of genes annotated by the differentially accessible
950 regions is indicated in brackets with brown font. DARs, differentially accessible regions.
951 **C)** The proportion and number of inflorescent-specific, seedling-specific and shared
952 differentially accessible regions among total differentially accessible regions identified
953 in the inflorescences and seedlings of each SWI/SNF mutant compared to the wild type.
954 DARs, differentially accessible regions. **D)** Heat map showing the pairwise Pearson
955 correlation coefficient based on the accessibility changes at the total genes with changed
956 accessibility in inflorescences of the displayed SWI/SNF mutants. **E)** Venn diagram
957 displaying the overlap of genes with down-regulated accessibility in inflorescences of

958 SAS mutants *syd*, *swi3d* and *sys1/2/3* compared to the wild type. **F)** Venn diagram
959 showing the overlap of genes with down-regulated accessibility in inflorescences of
960 *brm*, *syd* and *minu1/2* compared to the wild type. **G-I)** Line plots depicting the
961 enrichment of flower-specific expressed genes among the genes with down-regulated
962 accessibility in *brm* (**G**), *syd* (**H**) and *minu1/2* (**I**) as determined by GSEA analysis. The
963 grey regions represent the ranked list of the differences between the expression in
964 flowers and the average expression in all tissues of each *Arabidopsis* gene. The
965 normalized enrichment scores were labeled. *P* values were determined by permutation.
966 **J)** The proportion of genes showing up-regulated, down-regulated, and unchanged
967 expression among genes with down-regulated accessibility in the inflorescences of the
968 indicated SWI/SNF mutants relative to the wild type.

969 **Figure 3.** Effect of BAS, SAS, and MAS mutations on the accessibility of seedling-
970 specific and inflorescence-specific accessible regions. **A)** M (log ratio) versus A (log
971 average) (MA) plot showing the differential analysis results of ATAC-seq peaks in
972 inflorescences versus in seedlings of the wild-type plants. The plot shows the $\log_2$ (fold
973 change) and $\log_2$ (average reads concentration) of the ATAC-seq peaks. The red points
974 represent the significant changed peaks with FDR<0.05 and $|\log_2$ (fold change) $| \geq 0.5$.
975 **B)** The percentage of genes with down-regulated accessibility in the inflorescences of
976 indicated SWI/SNF mutants among the inflorescence-specific accessible genes. **C)** The
977 percentage of genes with down-regulated accessibility in the seedlings of indicated
978 SWI/SNF mutants among the seedling-specific accessible genes. **D)** Venn diagram
979 showing the overlap of the genes with consistently down-regulated accessibility in the
980 inflorescences of SAS mutants (*syd*, *swi3d*, and *sys1/2/3*) compared to the wild type
981 and the inflorescence-specific accessible genes. Gene set I represents the inflorescence-
982 specific accessible genes regulated by SAS, and gene set II represents the inflorescence-
983 specific accessible genes not regulated by SAS. **E)** Bubble plot showing the enriched
984 GO terms for gene set I and gene set II defined in (**D).** The size of the bubble represents
985 the gene number, and the color of the bubble represents the adjusted *P* value of the
986 enriched term. **F, G)** Profile plots depicting the ATAC-seq signals of the SWI/SNF

987 mutants and the wild-type plants in inflorescences and in seedlings at the genic regions
988 with inflorescence-specific accessibility (**F**) and the genic regions with seedling-
989 specific accessibility (**G**).

990 **Figure 4.** Specifically binding regions of BAS, SAS, and MAS in seedlings and
991 inflorescences. **A)** Heat map showing the pairwise Spearman correlation coefficients
992 based on the ChIP-seq read counts of the representative subunit of BAS (SWI3C), SAS
993 (SWI3D), and MAS (PMS2B) in seedlings (SDL) and inflorescences (IFL). **B)** Peak
994 number determined by ChIP-seq for the subunits of BAS, SAS and MAS in seedlings
995 and inflorescences. The number of genes annotated by the peaks is provided in brackets
996 with brown font. **C)** Number of seedling-specific and inflorescence-specific binding
997 peaks for the BAS, SAS and MAS subunits. The number of genes annotated by the
998 peaks is provided in brackets with brown font. **D)** Snapshot showing the ChIP-seq
999 signals of BAS, SAS and MAS subunits in inflorescences and seedlings at a genomic
1000 region. Blue peaks represent ChIP-seq signal in seedlings, and pink peaks represent
1001 ChIP-seq signal in inflorescences. Peaks marked with grey boxes indicate differential
1002 binding regions of BAS/SAS subunits between seedlings and inflorescences. Peaks
1003 marked with purple boxes indicate differential binding regions between the MAS
1004 subunit and the BAS/SAS subunits. The scale of normalized reads is shown. **E)** The
1005 proportion of regions annotated to specified chromatin features. The left two bars
1006 represent regions specifically bound by SAS in seedlings and inflorescences. Random:
1007 8,000 randomly selected genomic sites. **F, G)** Bubble plots showing the top 10 enriched
1008 GO terms in genes specifically bound by SAS in inflorescences (**F**) and in seedlings
1009 (**G**).

1010 **Figure 5.** Specific binding of SAS in inflorescence contributes to establishing the
1011 accessibility of flower development-related genes. **A)** The proportion of genes with
1012 down-regulated accessibility and maintained accessibility in the corresponding mutants
1013 among genes specifically bound by BAS, SAS and MAS in inflorescences (IFL) and in
1014 seedlings (SDL). **B, C)** Boxplots showing the enrichment of SAS in inflorescences (**B**)

1015 and the accessibility in the inflorescences of the wild-type plants (**C**) at the regions
1016 specifically bound by SAS in inflorescences with down-regulated accessibility (green)
1017 or maintained accessibility (pink) in the SAS mutant. The center lines and box edges of
1018 the box plots represents medians and the interquartile range (IQR), respectively.
1019 Whiskers extent within 1.5 times the IQR. *P* values were determined by two-tailed
1020 Mann-Whitney *U* test. **D)** Venn diagram showing the overlap between three gene sets:
1021 (I) genes specifically bound by SAS in inflorescences with decreased accessibility in
1022 the SAS mutant, (II) genes bound by SAS in both seedlings and inflorescences with
1023 decreased accessibility in the SAS mutant, and (III) inflorescence-specific accessible
1024 genes. Development-related genes selected from the overlap between gene sets I and
1025 III are listed below the Venn diagram. **E)** Snapshots displaying the ChIP-seq signal of
1026 the three SWI/SNF complexes and the ATAC-seq signal of SWI/SNF mutants in
1027 inflorescences and in seedlings at the genic region of genes involved in flower
1028 development. Blue represents the signal in seedlings, and pink represents the signal in
1029 inflorescences. Differential peaks of ChIP-seq and ATAC-seq in seedlings and
1030 inflorescences are marked by shadows. The scale of normalized reads is shown in each
1031 snapshot.

1032 **Figure 6.** Characterization of SAS-dependent accessible regions in inflorescences. **A)**
1033 The proportion of the BAS/SAS/MAS bound and unbound regions among regions with
1034 down-regulated accessibility in inflorescences of the core enzyme mutants of BAS,
1035 SAS and MAS. **B)** Pie chart showing the proportion of the peaks not bound by SAS (I),
1036 commonly bound by SAS in both seedlings and inflorescences (II) and specifically
1037 bound by SAS in inflorescences (III) among the total down-regulated peaks in the
1038 inflorescences of *swi3d* relative to the wild type. **C**, **D)** Boxplots showing the
1039 enrichment of SWI3D (**C**) and the accessibility in the inflorescences of the wild type
1040 plants (**D**) at the regions I, II and III defined in Fig. 5F. The center lines and box edges
1041 of the box plots represents medians and the interquartile range (IQR), respectively.
1042 Whiskers extend within 1.5 times the IQR. *P* values were determined by two-tailed
1043 Mann-Whitney *U* test. **E)** Heatmap exhibiting the different enrichment of the different

1044 enrichment of various motifs at the indicated regions. **F**) Bubble plot showing the ratio
1045 of the transcription factor (TF) binding peaks collected by the previous studies (Chen
1046 et al., 2018; van Mourik et al., 2023) among the 1,415 specific binding peaks of SWI3D.
1047 The binding peaks of TFs in inflorescences and seedlings are marked in purple and
1048 green, respectively.

1049 **Figure 7.** The binding of AP1 depends on the accessibility generated by SAS in
1050 inflorescences. **A**) Profile plots depicting the ATAC-seq signals in inflorescences of *ap1*,
1051 *syd* and the wild-type plants at the genic regions with down-regulated accessibility in
1052 *syd*. **B**) MA plot showing the differential analysis results of ATAC-seq peaks in
1053 inflorescences of *ap1* versus the wild-type plants. The plot shows the $\log_2$ (fold change)
1054 and $\log_2$ (average reads concentration) of the ATAC-seq peaks. The red points represent
1055 the significant changed peaks with FDR<0.05. **C)** Profile plots depicting the ChIP-seq
1056 signals of AP1-Flag in the background of wild-type and the *syd* mutant at the genic
1057 regions bound by AP1 in inflorescences. **D)** The percentage of the down-regulated
1058 accessible regions in *syd* overlapped with the AP1-bound regions and the percentage of
1059 the AP1-bound regions overlapped with the down-regulated accessible regions in *syd*.
1060 The number of the regions are marked on the bar plots. **E)** Boxplots showing the
1061 enrichment of AP1 in the wild type and the *syd* mutants at the AP1-bound regions, AP1-
1062 bound regions with down-regulated accessibility in syd and AP1-bound regions with
1063 maintained accessibility in *syd*, respectively. The center lines and box edges of the box
1064 plots represents medians and the interquartile range (IQR), respectively. Whiskers
1065 extent within 1.5 times the IQR. *P* values were determined by two-tailed Wilcoxon
1066 signed rank test. **F)** Snapshot demonstrating the ChIP-seq and ATAC-seq signals of the
1067 indicated samples at a genomic region. The down-regulated binding peaks of AP1 at
1068 the regions with down-regulated accessibility in SAS mutants are marked by the brown
1069 boxes. **G)** Snapshot demonstrating the ChIP-seq and ATAC-seq signals of the indicated
1070 samples at two genes targeted by AP1. In **(F)** and **(G)**, the scale of normalized reads is
1071 shown.

1072 **Supplemental information**

1073 **Supplemental Figure S1.** Inflorescence phenotype and different gene expression
1074 analysis in SWI/SNF mutants.

1075 **Supplemental Figure S2.** Proximal and distal accessible regions regulated by
1076 SWI/SNF complexes in seedlings and in inflorescences.

1077 **Supplemental Figure S3.** Characteristics of genes with down-regulated accessibility
1078 in inflorescences of SWI/SNF mutants.

1079 **Supplemental Figure S4.** GO enrichment of seedling-specific and inflorescence-
1080 specific accessible genes.

1081 **Supplemental Figure S5.** Effect of SWI/SNF subunit mutations on chromatin
1082 accessibility at inflorescence-specific accessible genes and seedling-specific accessible
1083 genes.

1084 **Supplemental Figure S6.** Comparison of the binding regions of BAS, SAS and MAS
1085 in seedlings and inflorescences.

1086 **Supplemental Figure S7.** Effect of *swi3d* mutation on accessibility and expression of
1087 inflorescence-specific accessible genes.

1088 **Supplemental Dataset 1.** Differentially expressed genes identified by RNA-seq in
1089 SWI/SNF mutants relative to wild type in inflorescences.

1090 **Supplemental Dataset 2.** Differentially accessible regions of SWI/SNF mutants
1091 identified by ATAC-seq in inflorescences.

1092 **Supplemental Dataset 3.** GO analysis of genes with decreased accessibility in
1093 SWI/SNF mutants identified by ATAC-seq.

1094 **Supplemental Dataset 4.** Differentially accessible regions of wild-type plants between
1095 inflorescences and seedlings.

1096 **Supplemental Dataset 5.** ChIP-seq peaks of SWI/SNF subunits in inflorescences and
1097 seedlings.

1098 **Supplemental Dataset 6.** Differentially binding regions of SWI/SNF subunits
1099 identified by ChIP-seq between inflorescence and seedlings.

1100 **Supplemental Dataset 7.** Transcription factor-binding motif analysis.

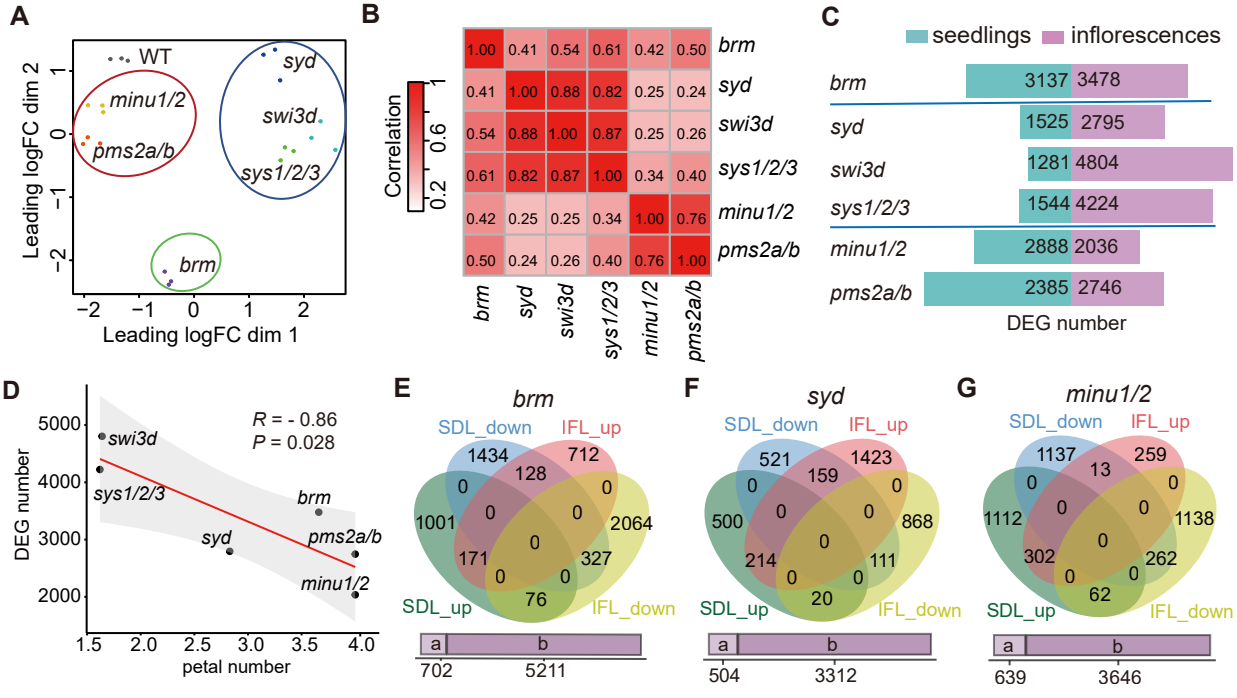

Figure 1. Comparison of DEGs identified by RNA-seq in SWI/SNF mutants between inflorescences and seedlings. **A)** MDS plot of the inflorescence RNA-seq samples. Clustering of BAS, SAS and MAS mutants are marked with green, blue, and red circles, respectively. **B)** Heat map showing the pairwise Pearson correlation coefficients based on the expression fold changes in inflorescences for the total DEGs of the displayed SWI/SNF mutants. **C)** The number of DEGs in SWI/SNF mutants relative to the wild type in both seedlings and inflorescences. **D)** The scatter plot showing the correlation between the average petal number (Guo et al., 2022) and the number of DEGs in inflorescences of the SWI/SNF mutants. A fitted regression line and a 95% confidence interval band are indicated. R represents the Pearson correlation coefficient. *P* value was determined by two-tailed *t* test. **E-G)** The overlap of up-regulated genes and down-regulated DEGs in seedlings and inflorescences of *brm* (**E**), *syd* (**F**) and *minu1/2* (**G**). The purple bars below the venn diagram marked by 'a' and 'b' represent genes shared by other sets and genes specifically belonging to one set of the venn diagrams, respectively.

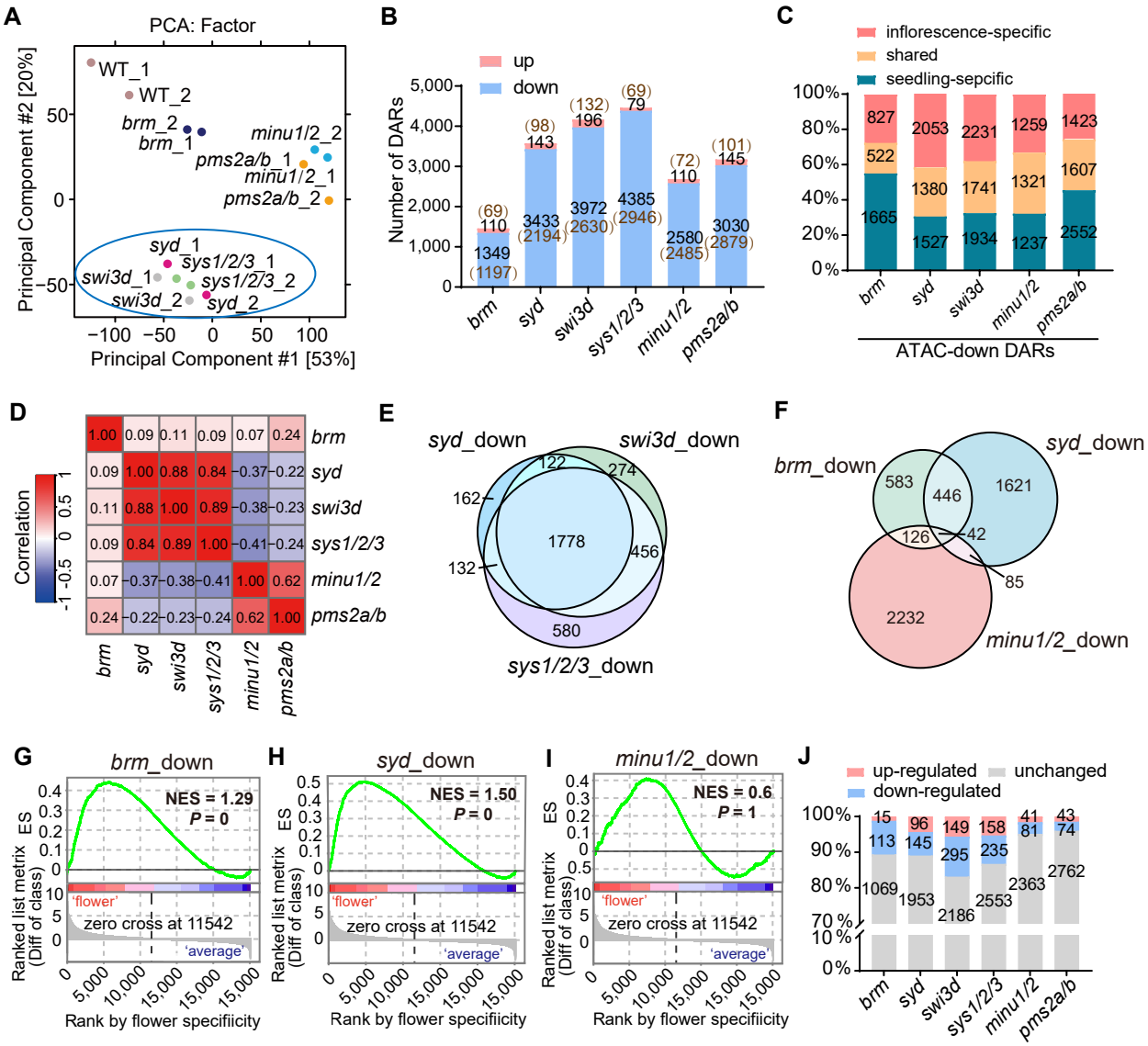

Figure 2. Analysis of differentially accessible regions in inflorescences of SWI/SNF mutants relative to the wild type. **A)** Principal component analysis (PCA) of the inflorescence ATAC-seq data of the wild type and SWI/SNF mutants. The cluster of SAS mutants are marked by the blue circle, respectively. **B)** The number of up-regulated and down-regulated differentially accessible regions in inflorescences of the SWI/SNF mutants identified by ATAC-seq. The number of genes annotated by the differentially accessible regions is indicated in brackets with brown font. DARs, differentially accessible regions. **C)** The proportion and number of inflorescent-specific, seedling-specific and shared differentially accessible regions among total differentially accessible regions identified in the inflorescences and seedlings of each SWI/SNF mutant compared to the wild type. DARs, differentially accessible regions. **D)** Heat map showing the pairwise Pearson correlation coefficient based on the accessibility changes at the total genes with changed accessibility in inflorescences of the displayed SWI/SNF mutants. **E)** Venn diagram displaying the overlap of genes with down-regulated accessibility in inflorescences of SAS mutants *syd*, *swi3d* and *sys1/2/3* compared to the wild type. **F)** Venn diagram showing the overlap of genes with down-regulated accessibility in inflorescences of *brm*, *syd* and *minu1/2* compared to the wild type. **G-I)** Line plots depicting the enrichment of flower-specific expressed genes among the genes with down-regulated accessibility in *brm* (**G**), *syd* (**H**) and *minu1/2* (**I**) as determined by GSEA analysis. The grey regions represent the ranked list of the differences between the expression in flowers and the average expression in all tissues of each Arabidopsis gene. The normalized enrichment scores were labeled. *P* values were determined by permutation. **J)** The proportion of genes showing up-regulated, down-regulated, and unchanged expression among genes with down-regulated accessibility in the inflorescences of the indicated SWI/SNF mutants relative to the wild type.

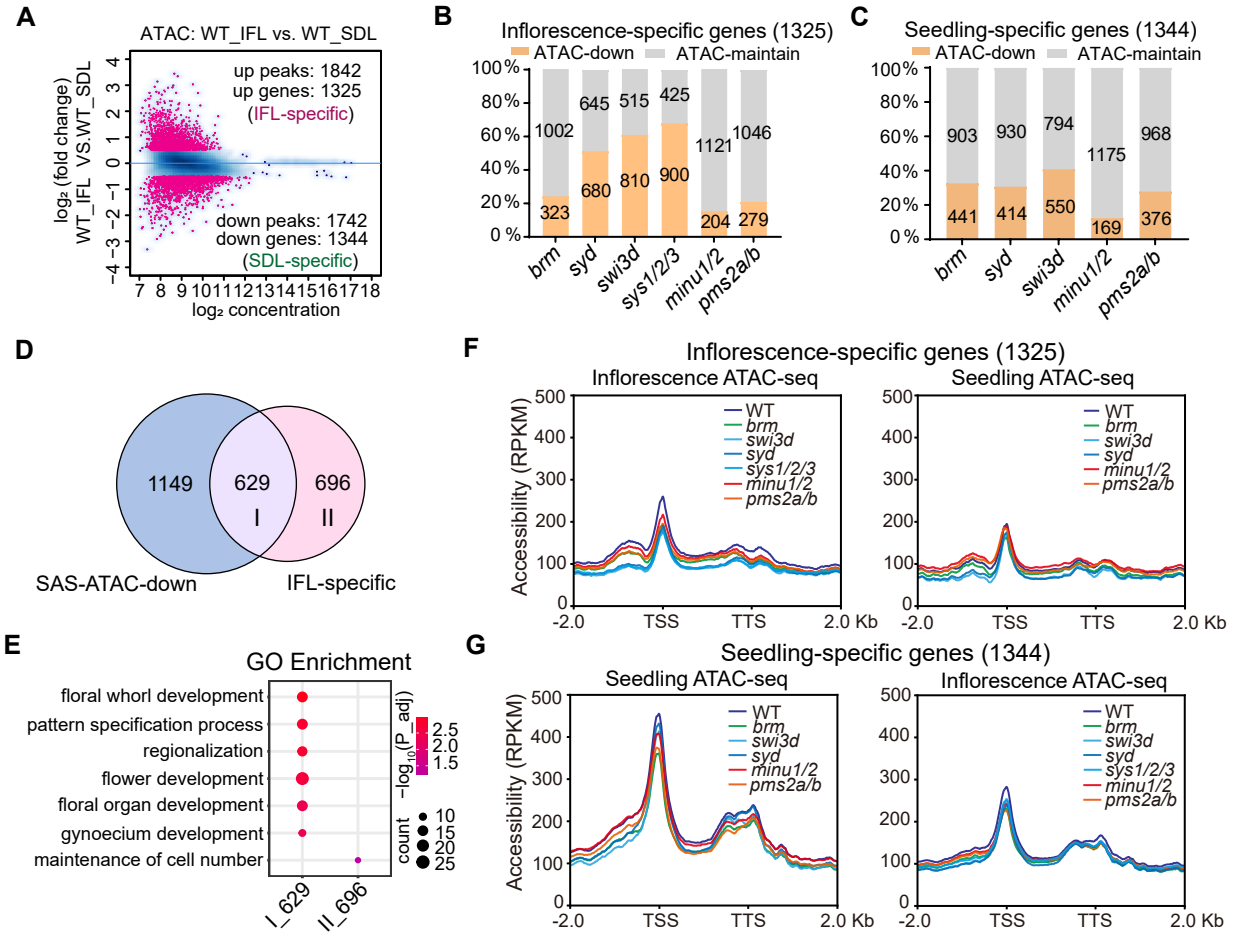

Figure 3. Effect of BAS, SAS, and MAS mutations on the accessibility of seedling-specific and inflorescence-specific accessible regions. **A)** M (log ratio) versus A (log average) (MA) plot showing the differential analysis results of ATAC-seq peaks in inflorescences versus in seedlings of the wild-type plants. The plot shows the $\log_2$ (fold change) and $\log_2$ (average reads concentration) of the ATAC-seq peaks. The red points represent the significant changed peaks with FDR<0.05 and $|\log_2 \text{(fold change)}| \geq 0.5$. **B)** The percentage of genes with down-regulated accessibility in the inflorescences of indicated SWI/SNF mutants among the inflorescence-specific accessible genes. **C)** The percentage of genes with down-regulated accessibility in the seedlings of indicated SWI/SNF mutants among the seedling-specific accessible genes. **D)** Venn diagram showing the overlap of the genes with consistently down-regulated accessibility in the inflorescences of SAS mutants (*syd*, *swi3d*, and *sys1/2/3*) compared to the wild type and the inflorescence-specific accessible genes. Gene set I represents the inflorescence-specific accessible genes regulated by SAS, and gene set II represents the inflorescence-specific accessible genes not regulated by SAS. **E)** Bubble plot showing the enriched GO terms for gene set I and gene set II defined in (**D**). The size of the bubble represents the gene number, and the color of the bubble represents the adjusted *P* value of the enriched term. **F, G)** Profile plots depicting the ATAC-seq signals of the SWI/SNF mutants and the wild-type plants in inflorescences and in seedlings at the genic regions with inflorescence-specific accessibility (**F**) and the genic regions with seedling-specific accessibility (**G**).

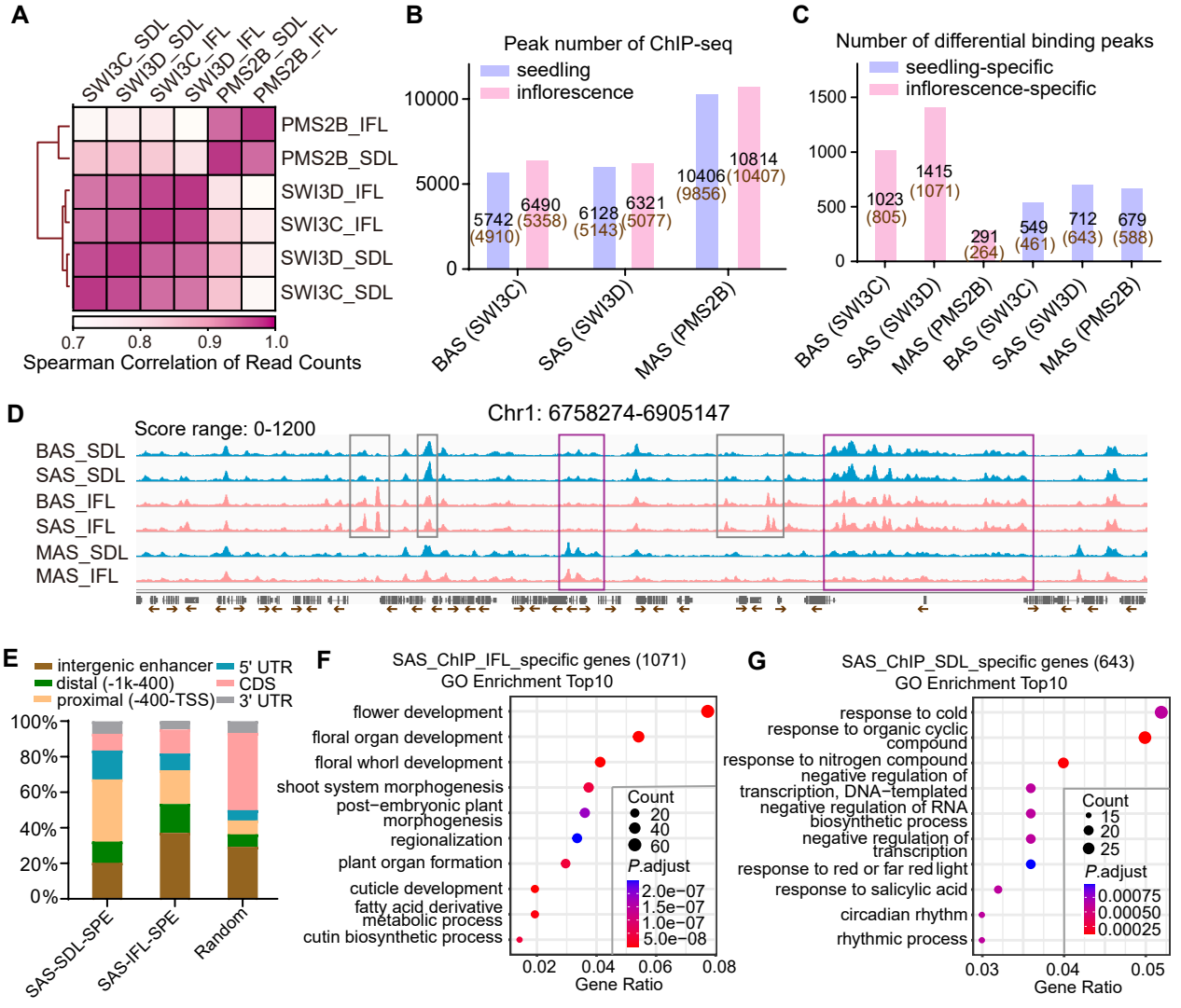

Figure 4. Specifically binding regions of BAS, SAS, and MAS in seedlings and inflorescences. **A)** Heat map showing the pairwise Spearman correlation coefficients based on the ChIP-seq read counts of the representative subunit of BAS (SWI3C), SAS (SWI3D), and MAS (PMS2B) in seedlings (SDL) and inflorescences (IFL). **B)** Peak number determined by ChIP-seq for the subunits of BAS, SAS and MAS in seedlings and inflorescences. The number of genes annotated by the peaks is provided in brackets with brown font. **C)** Number of seedling-specific and inflorescence-specific binding peaks for the BAS, SAS and MAS subunits. The number of genes annotated by the peaks is provided in brackets with brown font. **D)** Snapshot showing the ChIP-seq signals of BAS, SAS and MAS subunits in inflorescences and seedlings at a genomic region. Blue peaks represent ChIP-seq signal in seedlings, and pink peaks represent ChIP-seq signal in inflorescences. Peaks marked with grey boxes indicate differential binding regions of BAS/SAS subunits between seedlings and inflorescences. Peaks marked with purple boxes indicate differential binding regions between the MAS subunit and the BAS/SAS subunits. The scale of normalized reads is shown. **E)** The proportion of regions annotated to specified chromatin features. The left two bars represent regions specifically bound by SAS in seedlings and inflorescences. Random: 8,000 randomly selected genomic sites. **F, G)** Bubble plots showing the top 10 enriched GO terms in genes specifically bound by SAS in inflorescences (**F**) and in seedlings (**G**).

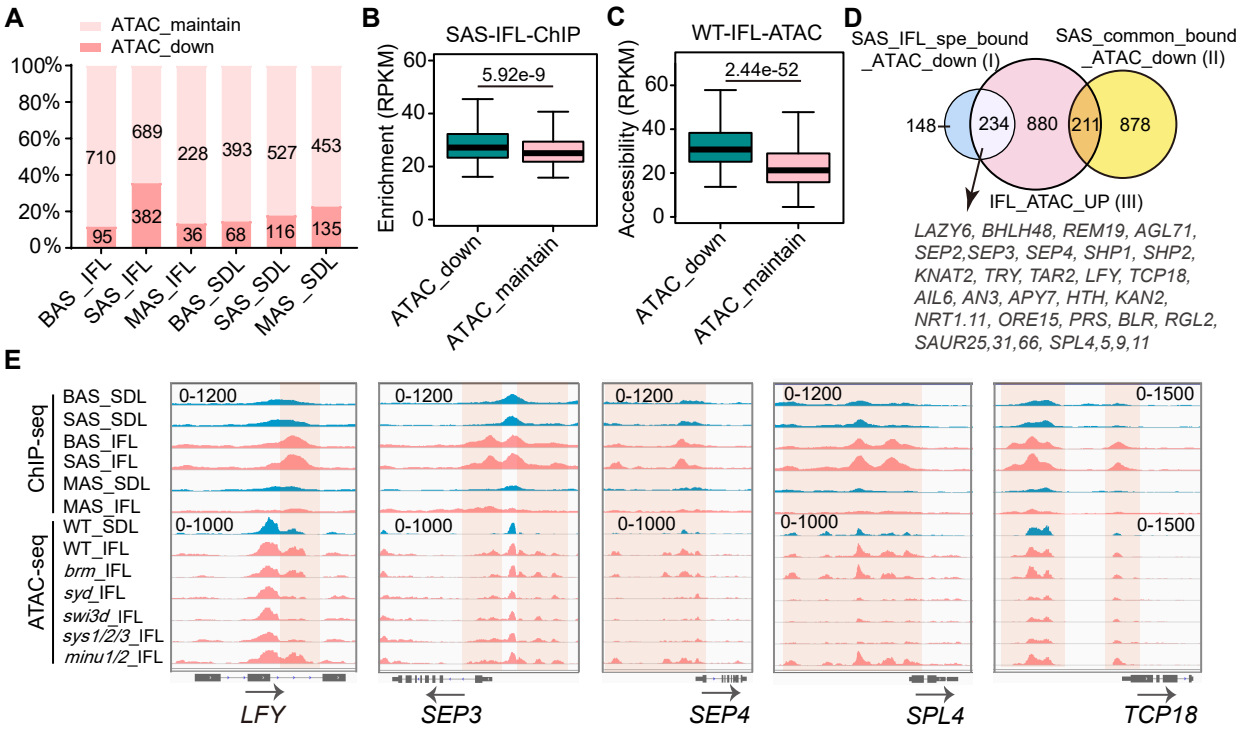

Figure 5. Specific binding of SAS in inflorescence contributes to establishing the accessibility of flower development-related genes. **A)** The proportion of genes with down-regulated accessibility and maintained accessibility in the corresponding mutants among genes specifically bound by BAS, SAS and MAS in inflorescences (IFL) and in seedlings (SDL). **B, C)** Boxplots showing the enrichment of SAS in inflorescences (**B**) and the accessibility in the inflorescences of the wild-type plants (**C**) at the regions specifically bound by SAS in inflorescences with down-regulated accessibility (green) or maintained accessibility (pink) in the SAS mutant. The center lines and box edges of the box plots represents medians and the interquartile range (IQR), respectively. Whiskers extent within 1.5 times the IQR. *P* values were determined by two-tailed Mann-Whitney *U* test. **D)** Venn diagram showing the overlap between three gene sets: (I) genes specifically bound by SAS in inflorescences with decreased accessibility in the SAS mutant, (II) genes bound by SAS in both seedlings and inflorescences with decreased accessibility in the SAS mutant, and (III) the inflorescence-specific accessible genes. Development-related genes selected from the overlap between gene sets I and III are listed below the Venn diagram. **E)** Snapshots displaying the ChIP-seq signal of the three SWI/SNF complexes and the ATAC-seq signal of SWI/SNF mutants in inflorescences and in seedlings at the genic region of genes involved in flower development. Blue represents the signal in seedlings, and pink represents the signal in inflorescences. Differential peaks of ChIP-seq and ATAC-seq in seedlings and inflorescences are marked by shadows. The scale of normalized reads is shown in each snapshot.

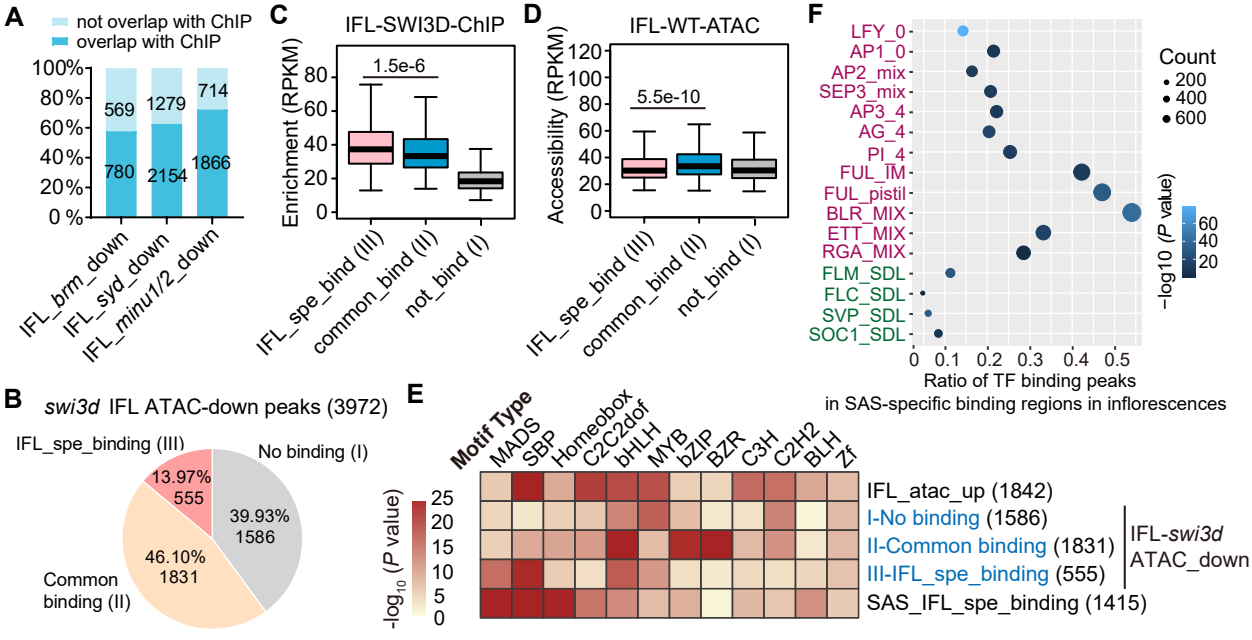

Figure 6. Characterization of SAS-dependent accessible regions in inflorescences. **A)** The proportion of the BAS/SAS/MAS bound and unbound regions among regions with down-regulated accessibility in inflorescences of the core enzyme mutants of BAS, SAS and MAS. **B)** Pie chart showing the proportion of the peaks not bound by SAS (I), commonly bound by SAS in both seedlings and inflorescences (II) and specifically bound by SAS in inflorescences (III) among the total down-regulated peaks in the inflorescences of swi3d relative to the wild type. **C, D)** Boxplots showing the enrichment of SWI3D (**C**) and the accessibility in the inflorescences of the wild-type plants (**D**) at the regions I, II and III defined in Figure 5F. The center lines and box edges of the box plots represents medians and the interquartile range (IQR), respectively. Whiskers extend within 1.5 times the IQR. P values were determined by two-tailed Mann-Whitney *U* test. **E)** Heatmap exhibiting the different enrichment of the different enrichment of various motifs at the indicated regions. **F)** Bubble plot showing the ratio of the transcription factor (TF) binding peaks collected by the previous studies (Chen et al., 2018; van Mourik et al., 2023) among the 1,415 specific binding peaks of SWI3D. The binding peaks of TFs in inflorescences and seedlings are marked in purple and green, respectively.

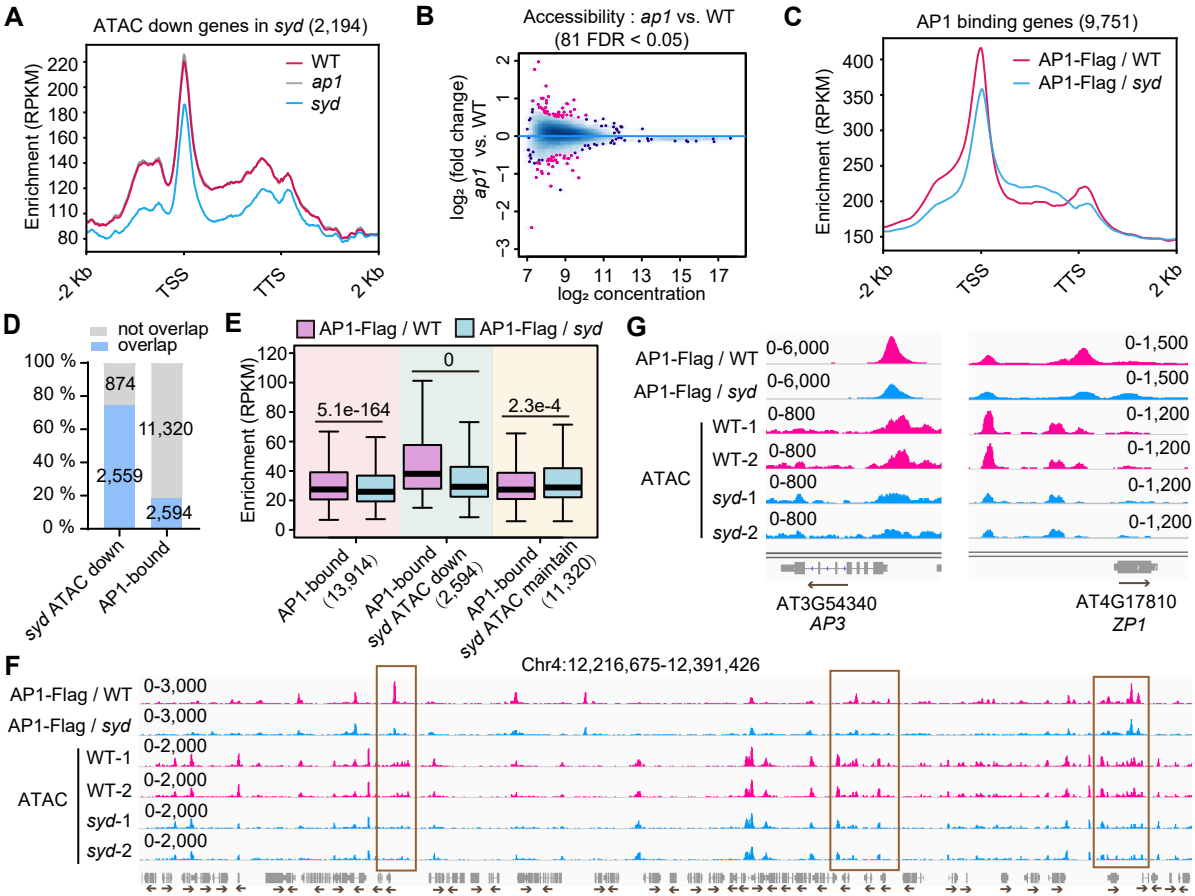

Figure 7 The binding of AP1 depends on the accessibility generated by SAS in inflorescences. **A)** Profile plots depicting the ATAC-seq signals in inflorescences of *ap1*, *syd* and the wild-type plants at the genic regions with down-regulated accessibility in *syd*. **B)** MA plot showing the differential analysis results of ATAC-seq peaks in inflorescences of *ap1* versus the wild-type plants. The plot shows the $\log_2$ (fold change) and $\log_2$ (average reads concentration) of the ATAC-seq peaks. The red points represent the significant changed peaks with FDR<0.05. **C)** Profile plots depicting the ChIP-seq signals of AP1-Flag in the background of wild-type and the *syd* mutant at the genic regions bound by AP1 in inflorescences. **D)** The percentage of the down-regulated accessible regions in *syd* overlapped with the AP1-bound regions and the percentage of the AP1-bound regions overlapped with the down-regulated accessible regions in *syd.* The number of the regions are marked on the bar plots. **E)** Boxplots showing the enrichment of AP1 in the wild type and the *syd* mutants at the AP1-bound regions, AP1-bound regions with down-regulated accessibility in *syd* and AP1-bound regions with maintained accessibility in *syd*, respectively. The center lines and box edges of the box plots represents medians and the interquartile range (IQR), respectively. Whiskers extent within 1.5 times the IQR. *P* values were determined by two-tailed Wilcoxon signed rank test. **F)** Snapshot demonstrating the ChIP-seq and ATAC-seq signals of the indicated samples at a genomic region. The down-regulated binding peaks of AP1 at the regions with down-regulated accessibility in SAS mutants are marked by the brown boxes. **G)** Snapshot demonstrating the ChIP-seq and ATAC-seq signals of the indicated samples at two genes targeted by AP1. In (**F**) and (**G**), the scale of normalized reads is shown.

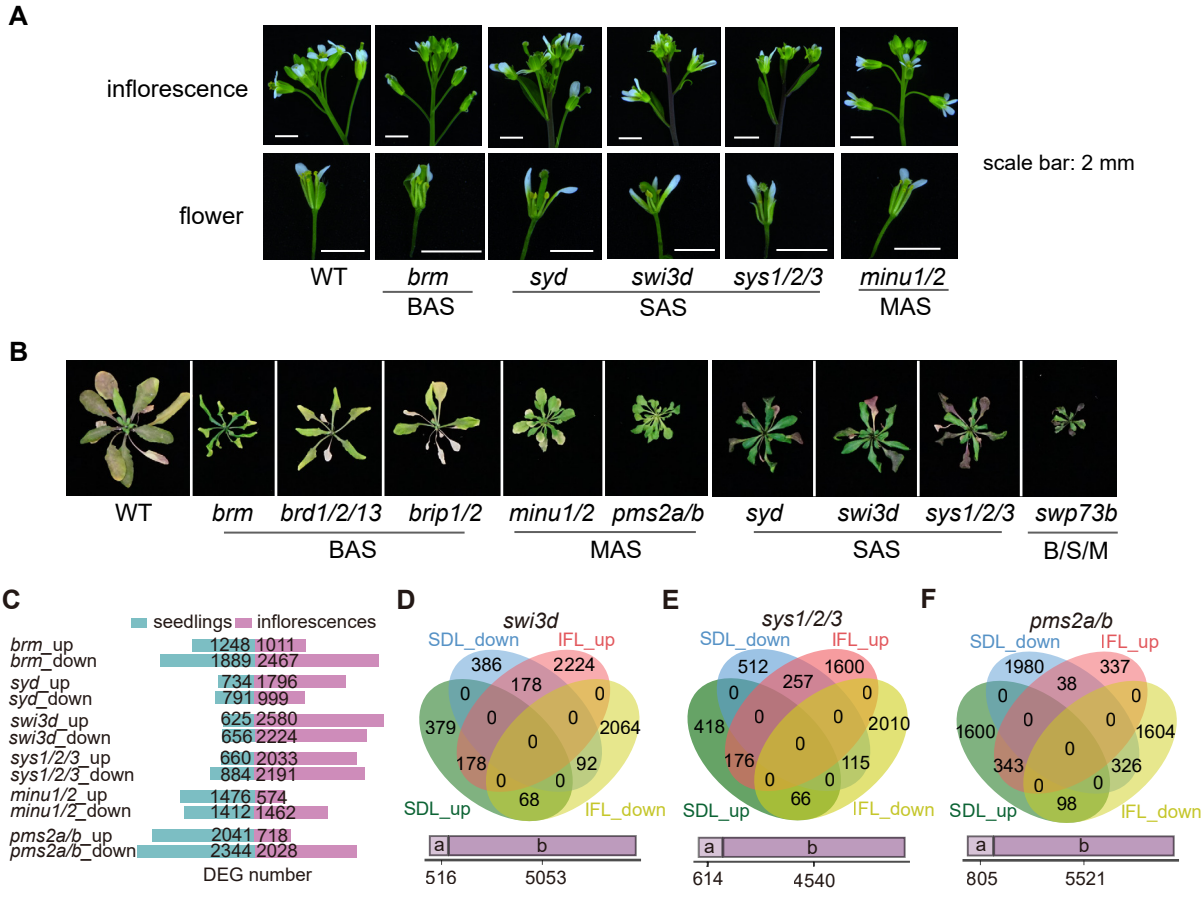

Supplemental Figure S1. Inflorescence phenotype and different gene expression analysis in SWI/SNF mutants. **A)** Photographs of inflorescences and flowers from 5~6-week-old SWI/SNF mutants. To show the inner stamens and pistil of a flower, some sepals and petals are removed in the second row of pictures. **B)** Images of rosette leaves from 8-week-old SWI/SNF mutants. To show the anthocyanin accumulation in rosette leaves, shoots and inflorescences were removed from the plant. **C)** The number of up-regulated and down-regulated DEGs in seedlings of inflorescences of SWI/SNF mutants, as determined by RNA-seq. **D-F)** Venn diagrams showing the overlap of up-regulated DEGs and down-regulated DEGs in seedlings and inflorescences of *swi3d* (**D**), *sys1/2/3* (**E**), and *pms2a/b* (**F**). The purple bar below the venn diagram marked by 'a' and 'b' represent genes shared by other sets and genes specifically belonging to one set of the venn diagrams, respectively.

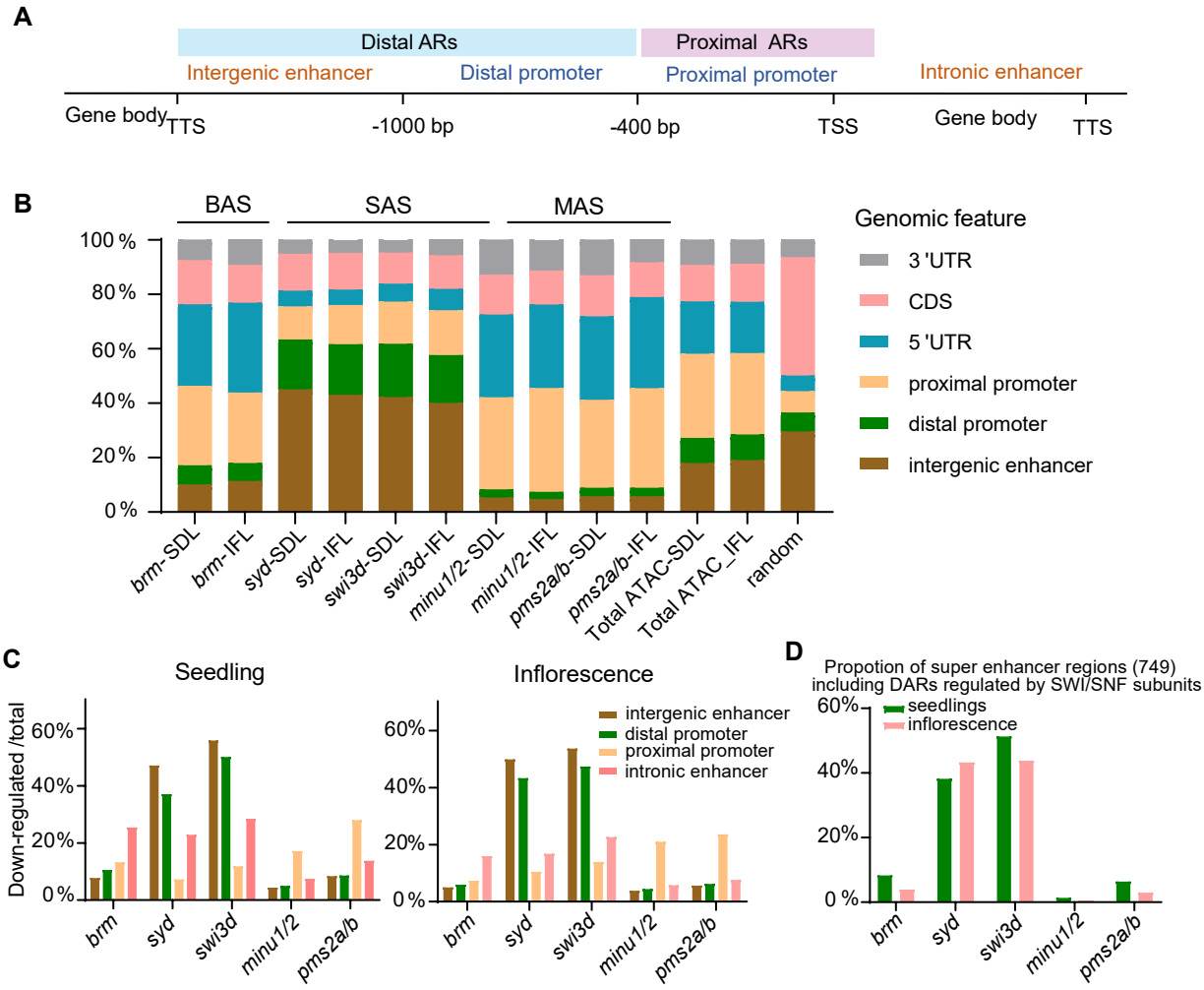

Supplemental Figure S2. Proximal and distal accessible regions regulated by SWI/SNF complexes in seedlings and in inflorescences. **A)** The illustration of specified genomic features used for the peak annotation. ARs, accessible regions. **B)** Proportion of down-regulated differentially accessible regions annotated to specified features to the total down-regulated differentially accessible regions in seedlings or inflorescences of the indicated SWI/SNF mutants. The proportion of accessible regions annotated to specified genomic features to total accessible regions identified by ATAC-seq in the seedlings and inflorescences of wild-type plants is also presented. Random: 8,000 random genomic sites. DARs, differentially accessible regions. **C)** Proportion of downregulated differentially accessible regions in each SWI/SNF mutant to the total accessible regions annotated to specified genomic features in seedlings and in inflorescences. **D)** The proportion of super enhancers including accessible regions regulated by SWI/SNF components in seedlings and in inflorescences to total super enhancers identified in a previous study (Zhao et al., 2022).

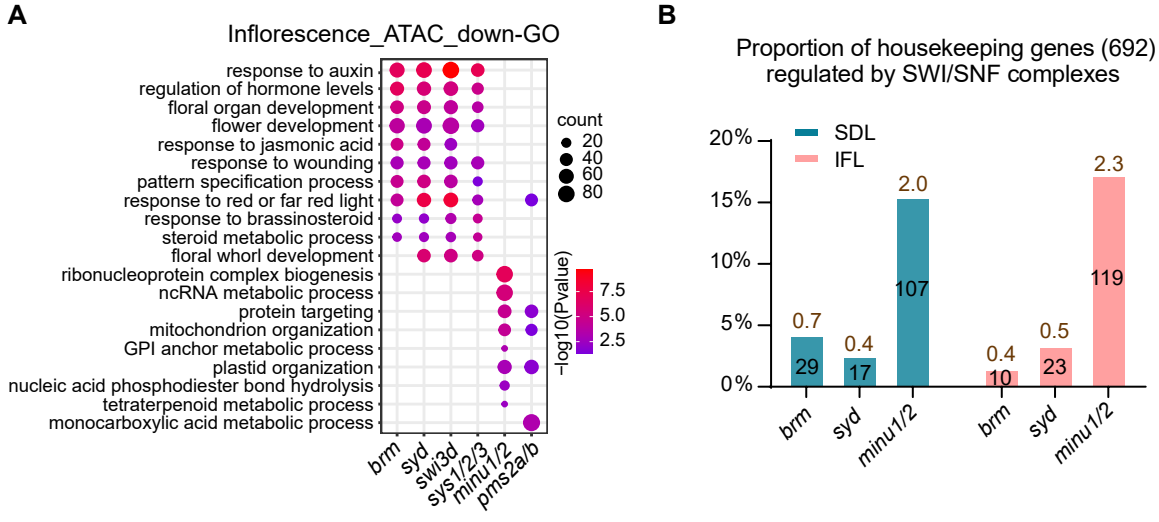

Supplemental Figure S3. Characteristics of genes with down-regulated accessibility in inflorescences of SWI/SNF mutants. **A)** GO enrichment of genes with down-regulated accessibility in inflorescences of SWI/SNF mutants. Bubble plots show the enriched GO terms in genes with down-regulated accessibility in inflorescences of SWI/SNF muants. **B)** The propotions of housekeeping genes (identified by Cheng et al., 2017) showing down-regulated accessibility in seedlings (SDL) and inflorescences (IFL) of the SWI/SNF mutants. The number of overlaping genes are marked on the bars with black font. The values marked by the brown font above the bars represent the Representative Factors (the number of overlaping genes divided by the expected number of overlaping genes drawn from two independent groups).

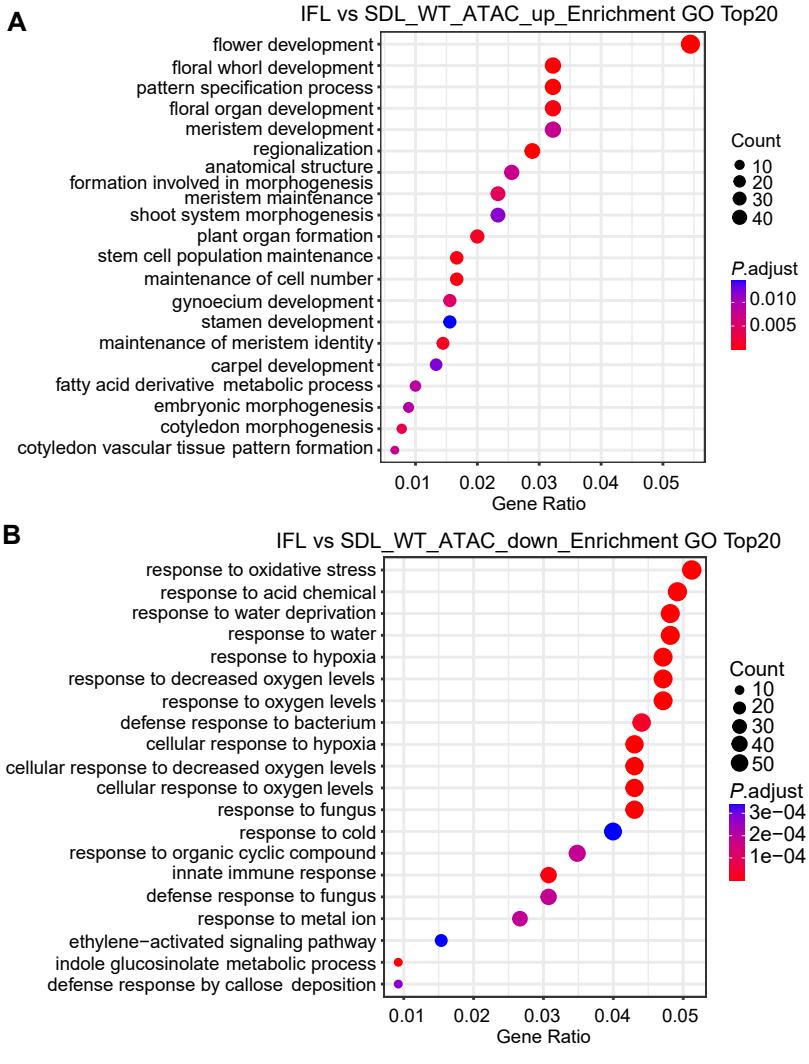

Supplemental Figure S4. GO enrichment of seedling-specific and inflorescence-specific accessible genes. **A, B)** Bubble plots showing the top 20 enriched GO terms in specific accessible genes in inflorescences (**A**) and seedlings (**B**) of wild-type plants.

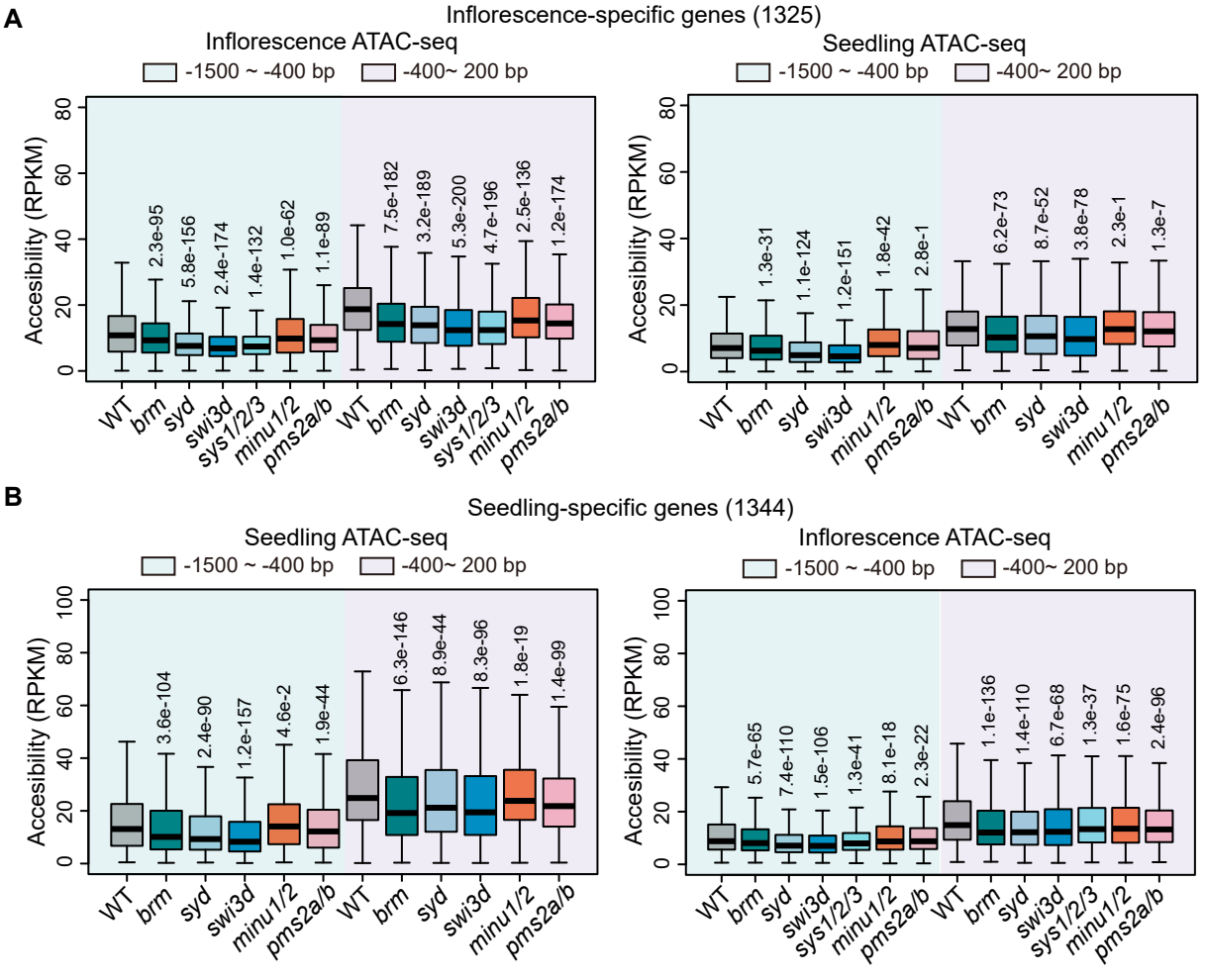

Supplemental Figure S5. Effects of SWI/SNF subunit mutations on chromatin accessibility at inflorescence-specific accessible genes and seedling-specific genes. **A, B)** Boxplots showing the chromatin accessibility levels in seedlings and inflorescences of the wild type and SWI/SNF mutants at the 400-1500 upstream region of TSS and at the -400-200 bp TSS-flanking region. Analysis was conducted separately for inflorescence-specific genes (**A**) and seedling-specific genes (**B**). The center lines and box edges of the box plots represents medians and the interquartile range (IQR), respectively. Whiskers extend within 1.5 times the IQR. *P* values were determined by two-tailed Wilcoxon signed rank test between the mutants and the wild-type control in each group.

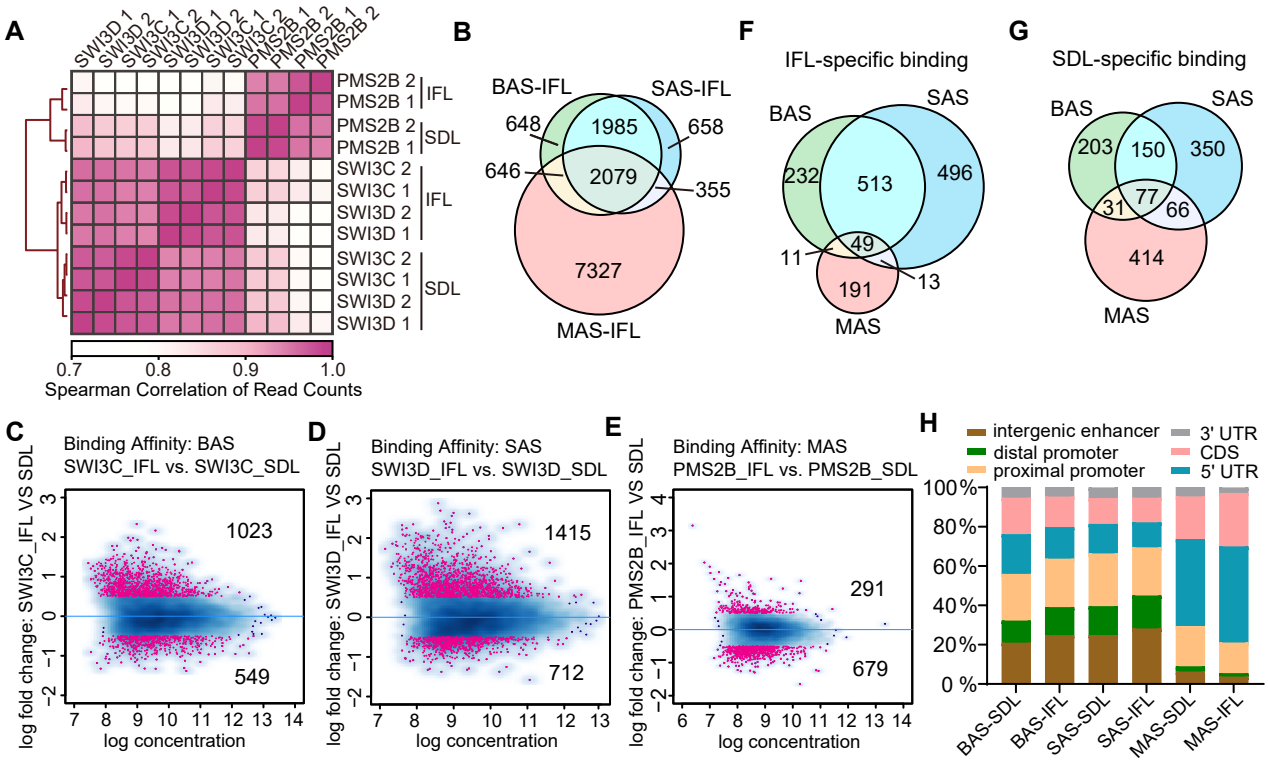

Supplemental Figure S6. Comparison of the binding regions of BAS, SAS and MAS in seedlings and inflorescences. **A)** Heat map showing the pairwise Spearman correlation coefficients based on the ChIP-seq read counts of the two replicates of BAS (SWI3C), SAS (SWI3D), and MAS (PMS2B) subunits in seedlings or in inflorescences. **B)** Venn diagram illustrating the overlap of the genes bound by BAS, SAS and MAS in inflorescences. **C-E)** MA plots showing the up-regulated and down-regulated binding peaks of the BAS (**C**), SAS (**D**) and MAS (**E**) subunits in inflorescences compared to seedlings. The red points represent significant changed peaks with FDR<0.05 and $|\log_2$ (fold change) $|$ >= 0.5. **F, G)** Venn diagrams showing the overlap of genes specifically bound by BAS, SAS and MAS in inflorescences (**F**) and in seedlings (**G**). **H)** The proportion of regions bound by BAS, SAS and MAS annotated to specified chromatin features in seedlings and in inflorescences. Random: 8,000 random genomic sites.

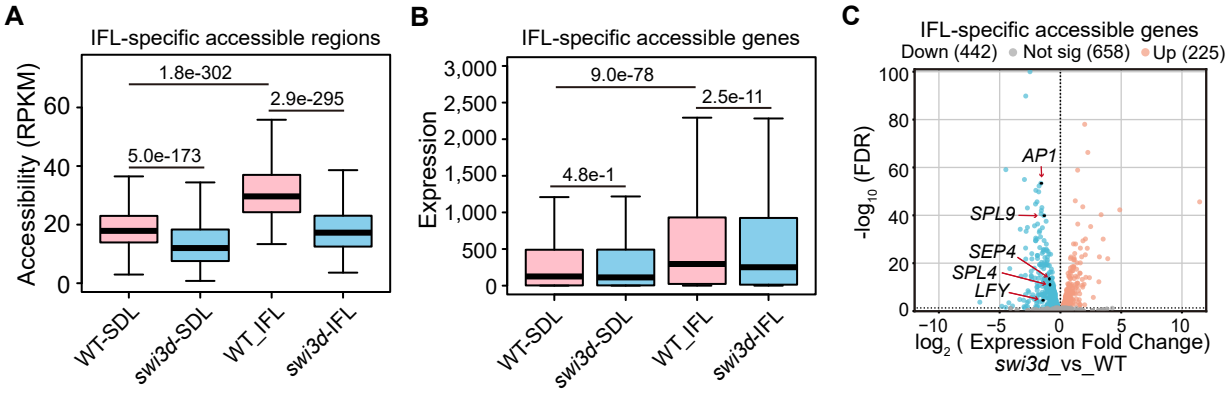

Supplemental Figure S7. Effects of *swi3d* mutation on accessibility and expression of inflorescence-specific accessible genes. **A)** Boxplots showing the accessibility of inflorescence-specific accessible regions in seedlings and inflorescences of the wild type and *swi3d* mutant. **B)** Boxplots displaying the expression levels of inflorescence-specific accessible genes in seedlings and inflorescences of the wild type and *swi3d* mutant. The center lines and box edges of the box plots represent medians and the interquartile range (IQR), respectively. Whiskers extend within 1.5 times the IQR. *P* values were determined by two-tailed Wilcoxon signed rank test. **C)** Volcano plot showing the differential expression of inflorescence-specific accessible genes in the *swi3d* mutant compared to the wild type. The fold change and FDR were calculated using the inflorescence RNA-seq data. Genes that are up-regulated in *swi3d* ($\log_2$(fold change)>0, FDR<0.05) are marked in red, genes that are down-regulated ($\log_2$(fold change)<0, FDR<0.05) are marked in blue, and genes that are not significantly differentially expressed (FDR<0.05) are marked in grey. Representative points are marked with gene names.